https://doi.org/10.5194/nhess-2021-79
Preprint. Discussion started: 23 March 2021

Natural Hazards and Earth System Sciences
Discussions

Flood-pedestrian simulator for modelling human response dynamics during flood-induced evacuation: Hillsborough stadium case study

Mohammad Shirvani[1], Georges Kesserwani[1]

[1]Department of Civil and Structural Engineering, University of Sheffield, Mappin St, Sheffield City Centre, Sheffield S1 3JD, UK

Correspondence to: Georges Kesserwani (g.kesserwani@sheffield.ac.uk)

Abstract. The flood-pedestrian simulator uses a parallel approach to couple a hydrodynamic model to a pedestrian model in a single agent-based modelling (ABM) framework using the Graphical Processing Units (GPU). It allows to dynamically exchange and process multiple agent information between the two models. The simulator is augmented with more realistic human-body characteristics and in-model behavioural rules. The new features are implemented in the pedestrian model to factor in age- and gender-related walking speeds for the pedestrians in dry zones with possible acceleration based on a maximum excitement condition. It is also adapted to use age-related moving speeds for pedestrians inside flooded zones, with either a walking condition or a running condition. The walking and running conditions are applicable without and with an existing two-way interaction condition that considers the effects of pedestrian congestion on the floodwater dynamics. A new autonomous change of direction condition is proposed to make way-finding decisions of pedestrians self-automated, based on the changes in the state of the floodwater dynamics or the most popular choice of destination selected by the other pedestrians. The relevance of the newly added characteristics and rules is demonstrated by applying the augmented simulator to reproduce a flood evacuation in a shopping centre test case, which was investigated with the version of the simulator that does not consider age and gender characteristics in the pedestrian model. The augmented simulator is finally applied to study evacuation scenarios for a mass evacuation from the Hillsborough football stadium located in a flood-prone area in Sheffield.

1 Introduction

Flooding can disturb local communities such as in and around urban hubs, putting people at risk (Flood and coastal erosion risk management policy statement, 2020). In lead-up to, and during, an urban flood people could be caught at different flood risk states depending on their body characteristics, individual actions, and interaction with the floodwater and each other (Environment Agency, 2006; Milanesi et al., 2015; Arrighi et al., 2017; Musolino et al., 2020; Moftakhari et al. 2018; Rufat et al., 2020; Hamilton et al., 2020). Understanding and quantifying how the interplay between people-related aspects affect flood risk to people is a desired way forward (Aerts et al., 2018). In the context of the flood risk management, methods and computational models have been developed to incorporate one or more of these aspects. This has been done with a particular

https://doi.org/10.5194/nhess-2021-79
Preprint. Discussion started: 23 March 2021


Natural Hazards and Earth System Sciences Discussions

focus on assessing and minimising the direct risks of floodwater on people, especially when they are under immediate evacuation condition. For this purpose, computer models have been used to evaluate evacuation strategies, including for the analysis of the potential variability in individual people's flood risk state, the lowest-risk pathways, and the time window for issuing an early warning (Aboelata and Bowloes, 2008; Lumbroso et al., 2011; Dawson et al., 2011; Mas et al., 2015; Liu and Lim, 2016; Bernardini et al., 2017; Zhu et al., 2019).

Most of the existing evacuation models are built upon the soft agent-based modelling (ABM) paradigm, as it offers the flexibility needed to represent both the interactive and the collective responses of people, either considered as moving individuals, groups of individuals in a vehicle, or household units (Zhuo and Han, 2020; Aerts, 2020). Incorporating these responses into ABM-based models enables to simulate people response dynamics into the flood risk analysis, leading to more informed predictions for flood adaptation planning and extraction of decision-relevant indicators (Aerts et al., 2018; McClymont et al., 2019). A two-dimensional hydrodynamic model is often used to feed information on the extent of the floodwater depth and velocity magnitude, as inputs, into ABM-based evacuation models from which the interactions between people and the floodwater could be modelled (Dawson et al., 2011; Bernardini et al., 2017; Aerts, 2020). These interactions directly affect the moving speed and stability states of people in and around the floodwater as they respond to an emergency warning while interacting with the features of an urban layout (Shirvani et al. 2020). The representation of these interactions within ABM-based models seems to require different levels of sophistication for the agent characteristics and behavioural rules depending on the purpose of the model design and the targeted scale of application.

For regional scale applications, ABM-based models were developed to simulate immediate crowd evacuation from a city, focusing on moving groups of individuals or household units using cars within a city road network to analyse response time of aware and unaware people to the immediate evacuation warning (Dawson et al., 2011; Mas et al., 2015; Liu and Lim, 2016; Zhu et al., 2019). These simulation models only consider vehicular emergency evacuation, which makes them not suited to simulate the interactive and the collective responses of moving individuals, or pedestrians, in and around small hubs (< 0.5 km × 0.5 km in size), such as shopping centres or sports venues. For such local scale applications, where pedestrians need to be individually modeled, only a few ABM-based evacuation models were reported. One of these models is the Life Safety Model (LSM, www.lifesafetymodel.net) developed by BC Hydro and HR Wallingford, which allows to analyse evacuation patterns of pedestrians along streetscapes and crossings (Lumbroso and Di Mauro, 2008; Lumbroso and Davison, 2018). Another model is LifeSIM (www.hec.usace.army.mil/software/hec-lifesim), developed by the US Army Corps of Engineers, which is capable of simulating individuals' responses to an emergency warning with the floodwater propagation, as they interact with the features of an urban layout, e.g. streetscapes and buildings (Aboelata and Bowles, 2008). These ABM-based evacuation models were developed to estimate the number of casualties and injuries and evacuation time, and to pinpoint highest-risk locations due to severe flood types, e.g. in the immediate aftermath of a dam-break or a tsunami wave where individual's decisions and actions have insignificant influence on the model outcomes. Less attention has been given to model the microscopic responses, down to the scale of the moving individuals, in and around flooded urban hubs for the most common flood types that would often lead to a low to moderate flood risk to people (Environment Agency, 2006).

https://doi.org/10.5194/nhess-2021-79
Preprint. Discussion started: 23 March 2021


Natural Hazards and Earth System Sciences Discussions

One first step to designing an ABM-based evacuation model capable of capturing microscopic responses at a small urban scale was taken by Bernardini et al. (2017), who developed FlooPEDS. In FlooPEDS, the standard social force model for pedestrian dynamics (Helbing and Molnar, 1995) was adapted to further model individuals' moving speed and stability states in floodwater. These states were implemented based on the experimental data and recommendations in Ishigaki et al. (2009), Chanson et al. (2014) and Matsuo et al. (2011), though individuals' way-finding decisions were solely influenced by behavioural rules of the social force model. The coupling with the hydrodynamic model was used to receive information on the changes in the floodwater conditions within the urban environment. However, FlooPEDS was reported to adopt a serial approach, by running one of the social force model and hydrodynamic model at a time, and a number of simplifications to alleviate runtime and dynamic memory costs, i.e. using uniform floodwater conditions on coarse subdomains, limiting the number of pedestrians up to 300 with uniform characteristics and the simulation time to less than 600 s (Bernardini et al., 2017). Given its serial approach to the coupling, FlooPEDS is not ideally suited to incorporate the dynamic feedback from the moving pedestrians onto the floodwater flow. Shirvani et al. (2021) developed a flood-pedestrian simulator by taking a parallel approach to achieve the dynamic coupling between the hydrodynamic model and the social force model, both being ABM-based and running from a single ABM-based framework, Flexible Large-scale Agent-based Modelling Environment for the GPU (FLAMEGPU). The flood-pedestrian simulator on the FLAMEGPU framework benefits from the computational speed-up and high dynamic memory capacity of the Graphics Processing Unit (GPU). The latter property allows it to employ as fine resolution and as large population size as needed with the hydrodynamic and pedestrian models, respectively (within the capacity of available GPU memory). This simulator is therefore supported with a two-way interaction condition to dynamically exchange agent information as they get updated across both the social force model and the hydrodynamic model. The two-way interaction condition allows to capture both the response of moving pedestrians to the floodwater and the back interaction of pedestrians' presence on the floodwater flow. Enabling the two-way interaction condition was found to significantly affect the model outcomes in and around congested areas: predict reduced flood risk for the pedestrians in low to medium risk areas and increased risk for those around high risk areas (Shirvani et al., 2021). In Shirvani et al. (2020), the social force model of the same simulator was further augmented with empirical datasets and experimentally derived formulas to incorporate non-uniform body characteristics and more variable moving speed and stability states of pedestrian agents in floodwater. The simulator was found to predict significantly prolonged evacuation times and higher number of at-risk pedestrians in low to medium risk areas in line with an increased sophistication in the pedestrian agent characteristics and behavioural rules (Shirvani et al., 2020), even without enabling the two-way interaction condition. In the latter version of the simulator, pedestrian agents were initialised to store body height and mass information, which were the only human body factors considered to influence the determination of their stability states in the floodwater; and, were assigned variable moving speeds that are solely based on the mechanics of the floodwater. Also, the latter version of the simulator was limited to assigning a way-finding decision for the pedestrian agents based on the availability of a fixed emergency exit destination (specified in advance), and did not explore the interplay between the two-way interaction condition and the pedestrian agent characteristics and rules.

https://doi.org/10.5194/nhess-2021-79
Preprint. Discussion started: 23 March 2021


Natural Hazards and Earth System Sciences Discussions

This paper presents the latest version of the simulator, augmented with new characteristics and rules for the pedestrian agents to more realistically represent the behaviour of people around and inside urban floodwater. In this version, pedestrian agents are initialised to store information of age, gender and more realistic body mass that are all accounted for within the rules determining both the moving speed and the stability states of the pedestrian agents inside the floodwater. The social force model is supplemented with empirically based age- and gender-related variable walking speeds to model the response of pedestrians in dry zones around the floodwater, and a new rule to incorporate a maximum excitement condition for replicating a faster than normal moving speed under evacuation condition. It is also supplemented with an experimentally derived formula to dynamically adapt moving speeds of pedestrian agents inside the floodwater that are also based on their age and gender, to include either a walking condition or a running condition. Each of these added rules could be applied with and without the two-way interaction condition. A new autonomous change of direction condition is proposed to enable the pedestrian agents to automatically make their way-finding decision informed by the state of the floodwater or the choices of pathways selected by their neighbouring agents. The added characteristics and behavioural rules are evaluated by analysing the associated changes induced in the simulated outcomes and also referring to the outcomes obtained from the latter version of the simulator. The utility of the simulator, with the new autonomous change of direction condition, is demonstrated to study evacuation scenarios for a mass evacuation from the Hillsborough football stadium in response to a flood emergency replicating the November 2019 Sheffield floods. Discussions of key findings and limitations are finally presented. Because the flood-pedestrian simulator is flexibly configurable to adopt other case studies and evacuation scenarios, its source code on the FLAMEGPU framework, including all the agent characteristics and/or rules, is made openly available (Shirvani and Kesserwani, 2021a), as well as the datasets from the simulated case studies (Shirvani and Kesserwani, 2021b) and a video supplement that visualises the simulations in real time (Shirvani, 2021).

2 Material and methods

2.1 Overview of the flood-pedestrian simulator

The flood-pedestrian simulator dynamically couples a hydrodynamic model to a pedestrian model within the same agent-based modelling (ABM) framework, FLAMEGPU (Shirvani et al., 2020; Shirvani et al., 2021). The pedestrian model adopts a standard social force model that accounts for the dynamic interactions occurring between moving pedestrians in a built environment (Li et al., 2019; Jiang et al., 2020). The pedestrians are represented by continuous space agents, each of which autonomously move in space and over time. The movement pattern of each pedestrian agent is derived by forces for avoiding collisions with their neighbouring pedestrian agents and with the key features within the environment layout, such as boundaries of the walkable area, terrain blocks and solid walls. The environment layout encodes force vector fields providing navigation to key destinations. These fields are stored within a grid of fixed discrete agents, forming a navigation map (Karmakharm et al., 2010). The navigation map is necessary for pedestrians' way-finding decisions while they are directed to reach their key destinations.

https://doi.org/10.5194/nhess-2021-79
Preprint. Discussion started: 23 March 2021


Natural Hazards and Earth System Sciences Discussions

The hydrodynamic model is applied on another fixed grid of discrete agents, flood agents, which is coincident with the grid of navigation agents. A flood agent stores information of the terrain properties in terms of height (z) and Manning's roughness parameter (n_M); and the state of floodwater variables in terms of depth (h) and velocity components (u and v). The state of floodwater variables is updated over time using a non-sequential computation of a hydrodynamic model that operates for all the flood agents at the same time. Each navigation agent thereby stores the updated state of floodwater variables from the coincident flood agent and translates it into a local flood hazard rating (HR) quantity. This HR quantity is estimated as HR = $(V + 0.5) \times h$ where V stands for the velocity magnitude, estimated as $V = \sqrt{u^2 + v^2}$, (Environment Agency, 2006). This HR quantity is usually used as a metric to assess the degree of flood risk to people (Kvočka et al., 2016; Willis et al., 2019; Costabile et al., 2020). Therefore, HR-related flood risk states are used based on the categorisation of flood risk to people reported in the UK Environment Agency (EA), as listed in Table 1.

Table 1: The flood risk states assigned for the pedestrian agents according to the HR ranges reported by the Environment Agency (2006)

HR range	Flood risk state
0.00 to 0.75	'Low' (safe for all)
0.75 to 1.50	'Medium' (danger for some, i.e. children)
1.50 to 2.50	'High' (danger for most)
2.50 to 20.0	'highest' (danger for all)

The navigation agents are set to act as a shared communication interface between the flood agents and pedestrian agents, where the information is dynamically exchanged between the three agents (Shirvani et al., 2021). This interaction mechanism allows a pedestrian agent to pick up a HR quantity from the navigation agent at its location and autonomously flag itself with one of the flood risk states listed in Table 1. Also, pedestrian agents are enabled to adapt their moving speed based on the change in the state of floodwater variables accessible from the navigation agents at its location and time.

The simulator is also supported with a functionality to enable a 'two-way interaction condition' to consider the effects that pedestrians' congestion would have on altering the floodwater hydrodynamics, which can be significant as shown in Arrighi et al. (2017) and Shirvani et al. (2021). Hence, this condition incorporates any local and temporal changes in the states of the floodwater variables in a flood agent as a result of increased accumulation of pedestrian agents over the navigation agent at its coincident location. By enabling this functionality, the navigation agent is set to count the number of pedestrian agents (N_p) that occupy its area at each time step. Then, the navigation agent uses N_p to alter local energy loss by locally updating n_M and passing it back to the coincident flood agent. The updated n_M is applied as $n_M^{updated} = n_M + (N_p \times n_M)$. The initial n_M parameter is set to be equal to 0.01 $s.m^{-1/3}$, representative of clear cement, and no more than 20 pedestrian agents are allowed to simultaneously occupy the area of a navigation agent, meaning that any local update in n_M cannot exceed 0.2 $m^{-1/3}$.

In the previous version of the simulator (Shirvani et al., 2020), the variable moving speed of pedestrian agents in floodwater was locally estimated based on an empirical formula that only considers the mechanics of floodwater depth and

https://doi.org/10.5194/nhess-2021-79
Preprint. Discussion started: 23 March 2021


Natural Hazards and Earth System Sciences Discussions

velocities (Bernardini et al., 2017). This formula does not take into account the impact of different age and gender groups on the moving speeds in both dry and flooded zones, and was therefore replaced with a more advanced set of moving speeds within the present version of the simulator (Sect. 2). Pedestrian agents were also featured with stability states to determine whether they can be mobile or immobile when they are inside the floodwater. The state of stability of the pedestrian agents was estimated based on two experimentally derived formulas (Xia et al. 2014). These formulas evaluate the incipient velocity limits (U_c) for toppling and sliding conditions of human subjects in the floodwater. The formulas are applied to each navigation agent by taking the body height and mass information of the pedestrian agent present at the navigation agent location, and also the states of floodwater variables at the coincident flood agent. The navigation agent then compares the incipient velocity to the magnitude of floodwater velocity (V). From this comparison, toppling and sliding stability states can be characterised for any pedestrian agent located at the navigation agent, as outlined in Table 2.

Table 2: The stability states of pedestrian agents in the flood-pedestrian simulator identified by comparing the incipient velocity limits (U_c) for toppling and sliding conditions to the velocity magnitude of floodwater (retrieved from Shirvani et al. (2020))

Condition	Stability state of a pedestrian agent in floodwater
$V < U_c^{(Toppling)}$ and $V < U_c^{(Sliding)}$	Stable condition - the pedestrian agent can have a moving speed
$V > U_c^{(Toppling)}$ and $V < U_c^{(Sliding)}$	Toppling-only condition - the pedestrian agent is immobilised
$V < U_c^{(Toppling)}$ and $V > U_c^{(Sliding)}$	Sliding-only condition - the pedestrian agent is immobilised
$V > U_c^{(Toppling)}$ and $V > U_c^{(Sliding)}$	Toppling-and-sliding condition - the pedestrian agent is immobilised

Note that the stability estimations in Table 2 were previously based on an empirical relationship for Body Mass Index (BMI) that only considers the body height of individual pedestrians (Shirvani et al., 2020). BMI ranges used in the present version of the simulator are based on age- and gender-related body mass characteristics (Sect. 2.2.1).

Finally, static-in-time destinations for the pedestrian agents were specified in the previous version of the simulator, such as entrance/exit doors taken as emergency exit during a flood evacuation in an indoor space (Shirvani et al., 2020). The pedestrian agents have therefore been fitted with new rules to enable the applicability of the simulator to study flood-induced pedestrian evacuation dynamics in an urban environment where there is no specific exit. These rules enable pedestrian agents to autonomously navigate to new pathways while the states of the floodwater change dynamically (Sect. 2.2.3).

2.2 New characteristics and rules for pedestrian agents

The pedestrian model was augmented to generate pedestrian agents with a random age and gender based on realistic datasets, that are also used to feature them with a set of randomised body mass (Sect. 2.2.1). More realistic ranges of moving speeds are also assigned to the pedestrian agents by considering their age and gender influences not only in dry zones but also in flooded zones (Sect. 2.2.2). New behavioural rules are also incorporated to enable pedestrian agents to alter their pathways and their choices for the emergency exit (Sec 2.2.3).

https://doi.org/10.5194/nhess-2021-79
Preprint. Discussion started: 23 March 2021

Natural Hazards and Earth System Sciences
Discussions

2.2.1 Age, gender, and body mass characterisation

Each pedestrian agent holds information of age, gender, and body mass at the time of its generation. To randomly assign an age, gender and body mass based on realistic distributions to each pedestrian, the UK national survey dataset (UK population by ethnicity, 2018) was used. As shown in Fig. 1, each pedestrian agent can have an age randomly selected from a range between 10 and 79 years old, and with a probability to keep the percentage of distribution of seven age groups. The excluded age groups, younger than 10 and older than 79 years old, make up 16 % of the UK population and represent children and elderly. To compensate for their exclusion, the percentage distribution of the other age groups was increased by around 2.3 %. Each pedestrian agent is also generated with a random 'male' or 'female' gender, each with equal chance of selection.

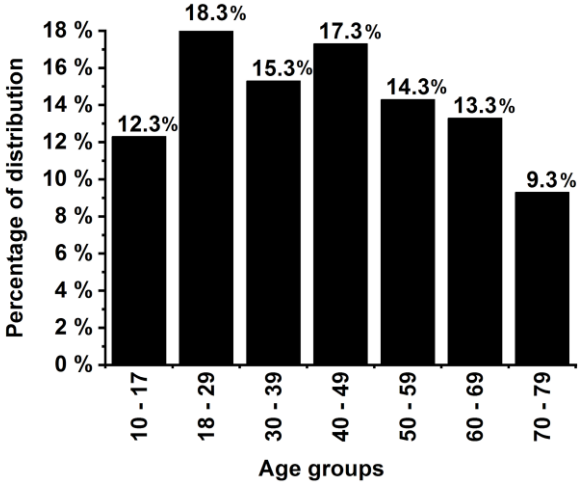

Figure 1: Age distribution assigned for the pedestrian agents in the flood-pedestrian simulator based on the UK's national survey (UK population by ethnicity, 2018)

Based on the age and gender of a pedestrian agent, its body mass, denoted by m_p (kg), is evaluated using the following formula (Disabled World, 2019):

$$m_p = l_p^2 \, BMI, \tag{1}$$

where l_p (m) stands for the body height of a pedestrian agent, which had already been incorporated within the previous version of the simulator (Shirvani et al., 2020). The BMI (kg / m^2) was randomly selected based on the ranges of age and gender listed in Table 3. For the age group between 10 and 17 years old, the BMI range was defined based on a standard for children (Prentice, 1998) and, based on samples of men and women who participated in the laboratory experiments reported in Bernardini et al. (2020) for the other age groups.

https://doi.org/10.5194/nhess-2021-79
Preprint. Discussion started: 23 March 2021


Natural Hazards and Earth System Sciences Discussions

Table 3: Ranges of BMI used according to gender and age of individuals (details in Prentice (1998) and Bernardini et al. (2020))

Age groups	Gender	BMI (kg / m^2)
10 to 17	Both	Between 18.5 and 24.9
18 to 29 30 to 39 40 to 49 50 to 59 60 to 69 70 to 79	Male	Between 18.21 and 32.10
	Female	Between 16.01 and 32.03

2.2.2 Variable moving speeds

Each pedestrian agent is enabled to evaluate their variable moving speed, age- and gender-related, based on two different sets of rules depending on whether the agent is located in a dry zone or in a flooded zone. To enable a pedestrian agent discern between dry zone and flooded zone, it resorts to the state of the floodwater's depth accessible from the navigation agent at its specific location and time.

A pedestrian agent that identifies a zero depth of floodwater is automatically flagged to be in a dry zone. These pedestrian agents are set to operate based on a 'dry-zone' moving speed rule under a walking condition. This rule assigns a randomly selected walking speed to a pedestrian agent from a set of predefined ranges that are classified according to different age and gender groups outlined in Table 4. The walking speed range of the 10-19 age group is defined according to the human's average walking speed and is the same for both male and female (Mohler et al., 2007; Toor et al., 2011). For pedestrian agents with 20 years of age and more, the ranges of their walking speed varies across different gender groups and are derived from an empirically identified standard proposed by Bohannon and Andrews (2011). As people are expected to move faster under evacuation conditions (Bernardini et al., 2020), pedestrian agents are applied an additional rule to increase their walking speed based on the 'maximum excitement condition' identified in the experiments of Bernardini and Qualiarimi (2020). This condition enables 'male' pedestrian agents to increase their walking speed by 60 % and 'female' agents to increase their walking speed by 76 %. The experimental findings of Lee et al. (2019) also suggest a faster maximum excitement condition for women, which may be associated with the fact that women have less tendency to be around floodwater compared to men (Becker et al., 2015; Hamilton et al., 2020).

Table 4: Ranges of walking speeds for the pedestrian agents located in dry zones according to their age and gender (Mohler et al., 2007; Toor et al., 2011; Bohannon and Andrews, 2011)

Age range (years)	Walking speed range (m/s)	
	Female	Male
10 to 19	1.39 to 1.47	1.39 to 1.47

https://doi.org/10.5194/nhess-2021-79
Preprint. Discussion started: 23 March 2021

Natural Hazards and Earth System Sciences Discussions

20 to 29	1.270 to 1.447	1.239 to 1.443
30 to 39	1.316 to 1.550	1.193 to 1.482
40 to 49	1.353 to 1.514	1.339 to 1.411
50 to 59	1.379 to 1.488	1.222 to 1.405
60 to 69	1.266 to 1.412	1.183 to 1.300
70 to 79	1.210 to 1.322	1.072 to 1.192

A pedestrian agent that identifies a non-zero depth of floodwater is automatically flagged to be in a flooded zone. These pedestrian agents are set to operate upon a 'flooded-zone' moving speed rule under either 'walking' or 'running' conditions. With this rule, each pedestrian is assigned a moving speed that is evaluated by an empirical formula extracted from the experiments in Bernardini et al. (2020). Denoting the moving speed of each individual by V_p (m/s), the formula reads

$$V_p = a.M^b, \quad (2)$$

where M is a function of specific force per width unit calculated by $M = \frac{V^2 h}{g} + \frac{h^2}{g}$ with h and V being the depth and the velocity magnitude of floodwater respectively, g is the gravitational constant and a and b are age-related parameters defining each of the 'walking' and 'running' conditions, which are listed in Table 5. M is estimated at the navigation agent, where the pedestrian agent is present, from copies of h and V obtained from the flood agent at the coincident location.

Table 5: The values of age-related parameters, a and b , identified by Bernardini et al. (2020) for evaluation of the moving speed of each individual under 'walking' and 'running' conditions via Eq. (2)

Age ranges (years)	Walking		Running	
	a	***b***	***a***	***b***
5 to 12	0.82	0.18	0.41	-0.21
13 to 20	0.54	-0.07	0.81	-0.19
21 to 28	0.36	-0.13	0.48	-0.19
29 to 36	0.35	-0.19	0.53	-0.23
37 to 44	0.43	-0.13	0.62	-0.20
45 to 52	0.57	-0.03	0.61	-0.17
53 to 60	0.32	-0.17	0.62	-0.20
61 to 68	0.16	-0.43	0.61	-0.17

The validity of Eq. (2) is limited to subjects under the age of 68 and only applicable to floodwater depths between 0.2 m to 0.7 m (Bernardini et al., 2020). In reality, floodwater depth can be outside these limits and it may happen that an elderly beyond 68 years of age is present in a flooded area. Therefore, extra rules were applied to extend the variety of moving speed of pedestrian agents in flooded zones beyond the aforementioned age and floodwater depth limits for Eq. (2):

- the moving speed of pedestrian agents with an age greater than 68 is evaluated by decreasing V_p of the 61-68 age group by 1.6 % per year, following the experimental findings of Dobbs et al. (1993),

https://doi.org/10.5194/nhess-2021-79
Preprint. Discussion started: 23 March 2021


Natural Hazards and Earth System Sciences Discussions

- pedestrian agents encountering a depth of floodwater shallower than 0.2 m are set to maintain dry-zone walking speed rule as they are not expected to experience significant interference from the floodwater on their walking speed (Lee et al., 2019), and
- pedestrian agents encountering floodwater greater than 0.7 m are given a moving speed informed by the stability limits reported in the UK's Flood Risks to People method (Environment Agency, 2006). Namely, these pedestrian agents are only set to have a moving speed when velocity magnitude V is less than 1.5 m/s, or otherwise, they remain immobile.

2.2.3 Autonomous change of direction condition

Each pedestrian agent is also featured with two extra rules to enable it to autonomously navigate into new pathways while moving within a flooded zone, where it encounters a non-zero floodwater depth from the navigation agent at its specific time and location. The first rule makes a pedestrian agent detect and choose another destination if the floodwater depth along its way becomes higher than a threshold of a floodwater depth to body height. The choice for the threshold is case-dependent and exploring many thresholds may be necessary (Sect. 3.3.2) as personal flood risk perception is uncertain and this affects the modelling of decisions, of when and where to enter the floodwater or make a move into another destination (Becker et al., 2015; Netzel et al., 2021). Applying this rule enables the pedestrian agents to make decisions on which pathway to take within an environment layout where there is no specific emergency exit at time of evacuation. The second rule applies to those pedestrian agents which remain undecided about selecting a pathway after a period of time (user-selected, Sect. 3.3.2). Such pedestrian agents are then set to detect the most popular destination chosen by the pedestrian agents within its surrounding. This rule is applied on the basis that group decisions have significant influence on the path finding decision of an individual in and around the floodwater (Becker et al., 2015; Lin et al., 2020).

2.3 Evaluation of the new characteristics and rules

The new characteristics and rules for pedestrian agents in the present version of the simulator were evaluated with a focus to assess their relevance for the analysis of pedestrian evacuation dynamics during a flood emergency (Sect. 2.3.1). Direct validation of agent-based models is a grand challenge as such models are aimed to study non-observable scenarios, where there is uncertainties associated with the emergent nature of behaviours and where validation datasets of such type are not available (An et al., 2020; Zhuo et al., 2020; Aerts 2020). One alternative approach is a component-wise validation (Bert et al., 2014). This approach was used at the development stage of the dynamically coupled hydrodynamic and pedestrian models within the simulator (Shirvani et al., 2021).

To validate the relevance of in-model behavioural rules, one suitable strategy is to Take A Previous Model and Add Something (TAPAS) (Polhill et al., 2010; Abebe et al. 2020). This strategy was previously applied by systematically increasing the level of sophistication of agent characteristics and rules, and running the simulator progressively to identify their relevance by analysing the respective changes to the simulation outcomes (Shirvani et al., 2020). The TAPAS approach is also applied

https://doi.org/10.5194/nhess-2021-79
Preprint. Discussion started: 23 March 2021


Natural Hazards and Earth System Sciences Discussions

here to evaluate the new characteristics and rules added to the present version of the simulator, by setting it up and running it for the same test case used in Shirvani et al. (2020), Sect. 2.3.1, for five different configuration modes that are summarised in Table 6.

Table 6: Configuration modes used to set up and run the simulator to evaluate the newly added characteristics and rules

Modes	Pedestrian behavioural rules				
	Two-way interaction	Moving speed in dry zones		Moving speed in flooded zone (Eq. (2))	
		Walking condition	Maximum excitement condition	Walking condition	Running condition
Mode 0	Disabled	Constant	Disabled	Age independent	Not applicable
Mode 1	Disabled	Age- and gender-related (Table 4)	Enabled (Sect. 2.2.2)	Age-related	Not applicable
Mode 2	Enabled				
Mode 3	Disabled			Not applicable	Age-related
Mode 4	Enabled				

The baseline Mode 0 retrieves the previous set up of the simulator (Shirvani et al., 2020), where pedestrian agents are only assigned a constant walking speed in dry zones and without the 'maximum excitement condition' (Sect. 2.2.2). In this mode, the pedestrian agents in flooded zones pick up a set of variable moving speeds under a 'walking' condition that is not age dependent. In addition to these, the 'two-way interaction' condition is also disabled (Sect. 2.1.1). Commonly in Mode 1 to 4, a random age- and gender-related walking speed is assigned to the pedestrian agents in dry zones (from Table 4). In Mode 1, the 'walking' condition (Sect. 2.2.2) is enabled, while Mode 2 allows to also take into account the 'two-way interaction' condition (Sect. 2.1.1). With Mode 3 and Mode 4, the 'running' condition (Sect. 2.2.2) is enabled instead, but only Mode 4 also enables the 'two-way interaction' condition (Sect. 2.1.1). The 'autonomous change of direction' condition is disabled with the simulation modes as the test case used in Shirvani et al. (2020) involves an evacuation of pedestrians in an indoor space where there is one specific emergency exit (Sect. 2.3.1). The latter condition will only be enabled for the real case study reported in Sect. 3 that involves an evacuation in an outdoor streetscape with many emergency exits.

2.3.1 Overview of the flood evacuation in a shopping centre test case

This test case was explored with the previous version of the flood-pedestrian simulator (Shirvani et al., 2020, Shirvani et al., 2021). It is reconsidered to assess the relevance of the new characteristics and rules added to the pedestrian agents within the present version of the simulator.

The test case considers a 332 × 332 m^2 hypothetical shopping centre that includes stores along its west and east sides, corridors and seven entrance/exit doors to the open space area (Fig. 2). The total walkable area of the shopping centre, including the open area and the corridors, is equal to 70,350.8 m^2. The pedestrian model within the simulator was set to have a constant

https://doi.org/10.5194/nhess-2021-79
Preprint. Discussion started: 23 March 2021

Natural Hazards and Earth System Sciences
Discussions

rate of 10 pedestrian agents entering or leaving from each of seven doors with an equal probability of one in seven. This set up maintains a constant number of 1,000 pedestrians wandering in the walkable area, when there is no floodwater. This number was selected to give an area of around 8.4 × 8.4 m^2 for each person using a calculator toolbox of the average space required for individuals in malls (Engineering ToolBox, 2003). The floodwater propagation was assumed to breach from the southern side along a 100 m opening (Fig. 2). When the floodwater starts to propagate, no more pedestrian agents are generated in the walkable area and the remaining ones are set to move to the emergency exit located at the northern side (Fig. 2), which was the only door open during the evacuation process.

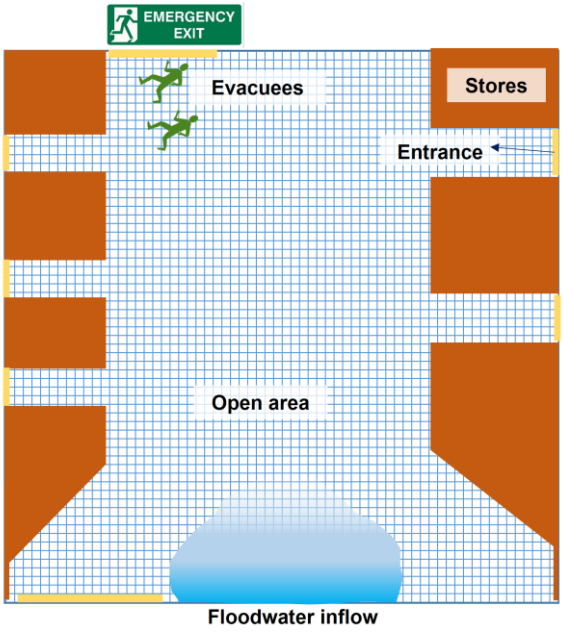

Figure 2: Sketch of the shopping centre: the meshed area in blue indicates the open area where pedestrians can walk to the entrance doors (coloured in yellow). Once the flood starts, evacuating pedestrians will go to the emergency exit (on the north side). The blocks in brown indicate terrain features assuming they are stores and the blue-shaded area in the southern part of the figure shows the location where the floodwater started to propagate.

The flooding inflow was generated based on an inflow hydrograph of a discharge, Q (m^3/s) propagating over a duration of 7.5 min, and peaking to 160 m^3/s at 3.75 min (Fig. 3). The hydrograph was produced based on the Norwich inundation case study, and because it results in a range for the HR that is inclusive of all the ranges listed in Table 1, i.e. HR < 7 (Shirvani et al., 2021). Deploying a hydrograph with shorter duration or a bigger peak would lead to significantly bigger HR, which is indicative of loss of life where a person does not have a chance to take an action and would immediately have a stability state under the sliding-only condition (hence is outside the scope of this study). When the floodwater starts to propagate over the walkable area, simulation time (t) of 0 min, the pedestrian agents start the evacuation and the simulation terminates when all the pedestrian agents have evacuated the walkable area.

https://doi.org/10.5194/nhess-2021-79
Preprint. Discussion started: 23 March 2021

Natural Hazards and Earth System Sciences
Discussions

326 The simulator was executed at a resolution of 2.59 m × 2.59 m for each of the grids of navigation and flood agents.
327 The time-step was taken to be the minimum between the adaptive time-step of the hydrodynamic model and the 1.0 s time-
328 step of the pedestrian model (a visualisation of the simulation can be found in the video supplement in Shirvani (2021)). In
329 each run, the simulator is set to record the information stored in the flood agents and the pedestrian agents at each time-step.
330 Recorded outputs from a simulation run include the positions of the pedestrian agents, their flood risk states (HR-related) and
331 or their stability states (with toppling-only condition and toppling-and-sliding conditions). Four runs were conducted based on
332 the configuration Mode 1 to Mode 4 (Table 6), and their recorded outputs are analysed next with respect to the baseline outputs
333 obtained from the run of the simulator with configuration Mode 0.

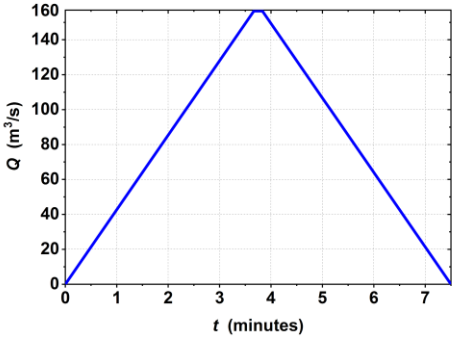

334

335 **Figure 3:** Inflow hydrograph that is used to generate the floodwater propagation from the southern side of the shopping centre

336 **2.3.2 Analysis of flood risks to people**

337 Figure 4a shows the number of evacuating pedestrians with a low flood risk state (HR < 0.75) predicted by the simulator using
338 all the configuration modes (Table 6). Figure 4a-left includes the evacuation patterns predicted by enabling the walking
339 condition for the age-related moving speeds (Mode 1) versus those predicted by further enabling the two-way interaction
340 condition (Mode 2). In Mode 1, the evacuation patterns are in good agreement with the baseline predictions (Mode 0, with
341 non-age related moving speeds) at flooding times when there are less than 50 pedestrians in the surrounding with a low flood
342 risk state, during 3.5 min to 6 min. Differences among the predictions start to occur when more than 150 pedestrians were
343 present, at 2 min and 8 min. This difference seems to impact the overall prediction, leading to an evacuation time that is 6 min
344 longer and a higher number of pedestrians being predicted to be under this flood risk state, during 8 min to 20 min. In Mode
345 2, compared to Mode 1, the number of evacuating pedestrians is seen to reduce further at flooding times involving more than
346 150 pedestrians, at 2 min and 10 min. This is expected as the more the crowding of pedestrians the more the energy loss in the
347 floodwater dynamics for low risk floodwaters, which in turn enables the pedestrians located behind to take a faster moving
348 speed. Figure 4a-right includes the evacuation patterns predicted by activating the running condition for the age-related moving
349 speeds (Mode 3), and those predicted by also enabling the two-way interaction condition (Mode 4). In Mode 3 and Mode 4,
350 the evacuation time decreased significantly (by almost 67 %) leading to evacuation patterns that are close to the baseline

https://doi.org/10.5194/nhess-2021-79
Preprint. Discussion started: 23 March 2021


Natural Hazards and Earth System Sciences Discussions

predictions (Mode 0). With Mode 3, discrepancies only occur after 2 min of flooding and after 8 min when there are more than 200 pedestrians moving based on the running condition. In Mode 4, the evacuation patterns remain close to those predicted under Mode 3, except at flooding times involving more than 200 pedestrians, at 2 min and 8 min. Overall, using the age-related moving speed with the walking condition and without or with the two-way interactions condition (Mode 1 or Mode 2) predicts longer evacuation patterns for pedestrians in a low flood risk state compared to the other three modes that lead to close patterns (Mode 0, Mode 3 and Mode 4). This condition seems useful to use with the simulator to study mass evacuation planning scenarios under low risk flooding. With the two-way interaction condition, slightly accelerated evacuation patterns should be expected at the times of the flooding when crowding occurs for pedestrians with a low flood risk state.

Figure 4b shows the number of evacuating pedestrians under a medium flood risk state ($0.75 < HR < 1.5$). With Mode 1, compared to Mode 0, a faster evacuation pattern is observed until 6 min before the number of pedestrians becomes 300. This suggests that before crowding occurs, pedestrians with a medium flood risk state are predicted to evacuate faster with Mode 1. However, when the number of pedestrians becomes more than 300, during 6 min to 8 min, Mode 1 leads to a slightly slower evacuation as observed previously with the pedestrians under a low flood risk state (compare Fig. 4a-left and Fig. 4b-left). This difference is not observed for the evacuation patterns predicted by the simulator with Mode 2, which leads to a number of pedestrians that does not exceed those observed with Mode 0. By using instead the age-related running condition under Mode 3 (Fig. 4b-right), no major changes can be observed in the evacuation patterns for the pedestrians with a medium flood risk state (compared to with Mode 0). Further enabling the two-way interaction condition (Mode 4) induces a slight reduction in the predicted number of pedestrians during the flooding time when the crowding is at its peak (Fig. 4b-right). As for the evacuation speed, it is predicted to be the same with all the modes for the pedestrians under a medium flood risk state. However, Mode 0 should be avoided as it can lead to the simulator predicting less pedestrians in this risk category, in particular at early flooding times before crowding occurs (compare the evacuation patterns in Fig. 4b during 2 min to 6 min). Hence, running the simulator with any of the configuration Mode 1 to Mode 4 does not seem to yield a major difference in the evacuation patterns for pedestrians with a medium flood risk state.

Figure 4c shows the number of evacuating pedestrians predicted to be under a high flood risk state ($1.5 < HR < 2.5$). For pedestrians with this risk category, running the simulator with any of the Mode 1 to Mode 4 lead to major differences in the evacuation patterns compared to those predicted under Mode 0. With Mode 1 to Mode 4, only a handful of pedestrians are predicted to have a high flood risk state, during 3 min to 5 min of the flooding, in contrast to what the simulator's prediction with Mode 0 suggests: up to 140 pedestrians within a time window of 4 min. Hence, using the age-related moving speed, under either the walking condition or the running condition, seems to make a difference in the predicted evacuation patterns of pedestrians with a high flood risk state. The impact of the two-way interaction condition on the evacuation pattern of such pedestrians can be detected by analysing the difference between the predictions made under Mode 1 vs. Mode 2, for the age-related walking condition (Fig. 4c-left), and between Mode 3 vs. Mode 4, for the age-related running condition (Fig. 4c-right). As can be seen, only a slightly higher number of pedestrians with a high flood risk state are predicted when the two-way interaction condition is also enabled, suggesting that it would not lead to a major difference in this case.

https://doi.org/10.5194/nhess-2021-79
Preprint. Discussion started: 23 March 2021

Natural Hazards and Earth System Sciences
Discussions

Figure 4d shows the number of evacuating pedestrians predicted to have a highest flood risk state (2.5 < HR < 20). In this case, with any of the Mode 1 to Mode 4, the simulator predicts these pedestrians to be at earlier times in the flooding compared to Mode 0. This implies that using the age-related moving speeds can provide a better prediction of the timing when the evacuating pedestrians would be at the highest flood risk state. The evacuation patterns predicted by the simulator using Mode 1 and Mode 3 are similar, indicating any of the running or walking conditions would lead to similar outcomes to inform on evacuating pedestrians with a highest flood risk state. However, the walking condition combined with the two-way interaction condition (Mode 2) leads to slightly higher number of pedestrians with this flood risk state, as these pedestrians would be more affected by the local changes induced the floodwater dynamics from those pedestrians, with a low risk state, crowding ahead (Shirvani et al., 2021). The running condition combined with the two-way interaction condition (Mode 4) does not lead to major changes in the evacuation patterns compared to the predictions with Mode 2. Hence, Mode 2 seems to be a sensible choice to use with the simulator to plan evacuation case studies involving severe flooding scenarios too.

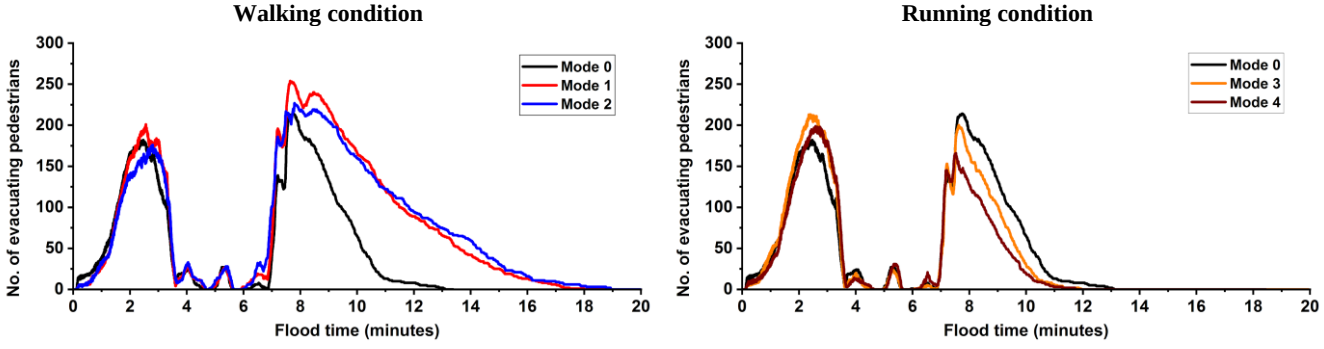

(a) Evacuating pedestrians with a low flood risk state (HR < 0.75)

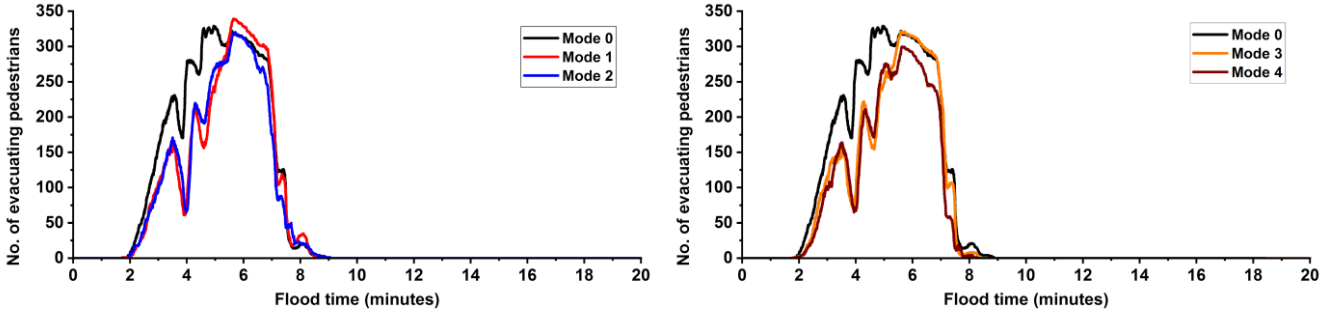

(b) Evacuating pedestrians with a medium flood risk state (0.75 < HR <1.5)

https://doi.org/10.5194/nhess-2021-79
Preprint. Discussion started: 23 March 2021

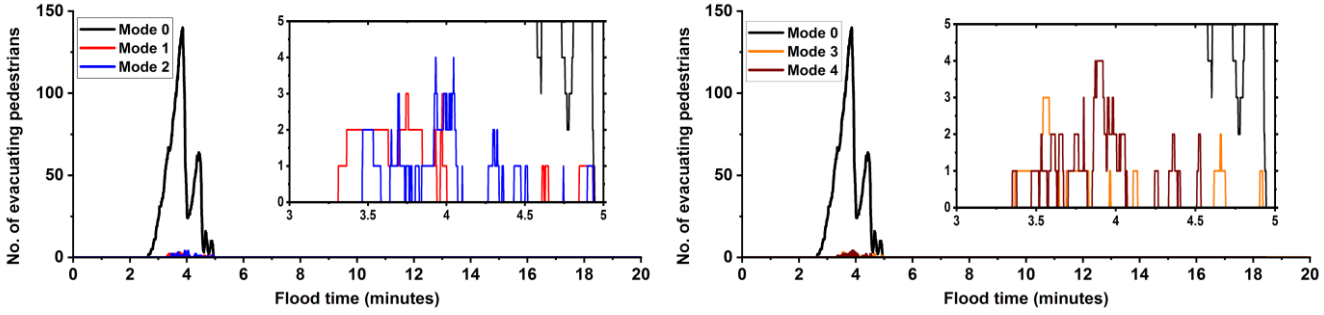

(c) Evacuating pedestrians with a high flood risk state (1.5 < HR < 2.5)

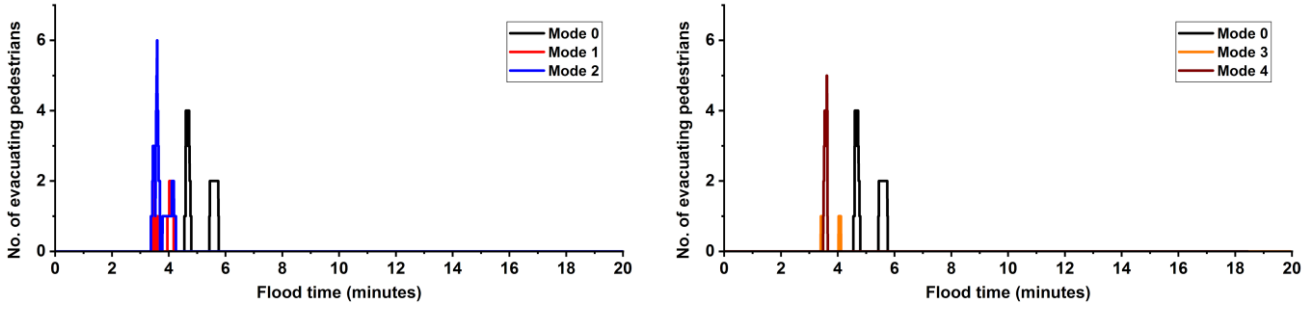

(d) Evacuating pedestrians with a highest flood risk state (2.5 < HR < 20)

Figure 4: Number of evacuating pedestrians predicted by the simulator under Mode 0 (baseline outcomes from the previous version of the simulator, Shirvani et al., 2020); Mode 1 or Mode 2 (age-related walking condition for the moving speeds without or with the two-way interaction condition); and Mode 3 or Mode 4 (age-related running condition for the moving speeds without/with the two-way interaction condition). Analysis is presented in sub-figures (a)-(d), each considering a different flood risk state.

Figure 5 contains the stability states of the pedestrians, plotted in terms of the number of evacuating pedestrians with a toppling-only condition (Fig. 5a) and with a toppling-and-sliding condition (Fig. 5b). The stability states are shown for the simulator predictions obtained by enabling the walking condition without or with the two-way interaction condition (Mode 1 or Mode 2), and by enabling the running condition without or with the two-way interaction condition (Mode 3 or Mode 4). The baseline predictions for the pedestrians' stability states obtained under Mode 0 are also included. With Mode 1 and Mode 3, the number of pedestrians predicted to be with a toppling-only condition and with a toppling-and-sliding condition are very similar to the baseline predictions. The pedestrians with such stability states were detected during 2 min to 8 min for the toppling-only condition, and during 2 min to 6 min for the toppling-and-sliding condition. As explored in Fig. 4, evacuating pedestrians with a low to medium flood risk state could be detected during 2 min to 8 min. Hence, using the simulator with the age-related moving speeds (Mode 1 or Mode 3) lead to similar information on the stability states even when the pedestrians have a low to medium flood risk state. With the two-way interaction condition (Mode 2 or Mode 4), less pedestrians were predicted to be with toppling-only and toppling-and-sliding conditions, namely when crowding occurs after 4.6 min, where there is a notable reduction in the number of pedestrians with a toppling-and-sliding condition (see also Fig. 6). Hence, the

https://doi.org/10.5194/nhess-2021-79
Preprint. Discussion started: 23 March 2021

Natural Hazards and Earth System Sciences
Discussions

activation of the two-way interaction condition predicts a lower number of pedestrians immobilised by the floodwater, namely when the walkable area involves localised crowding of pedestrians. This can also be observed in Fig. 6 that contrasts 2D spatial distributions of the evacuating pedestrians obtained with and without the two-way interaction condition (Mode 1 vs. Mode 2 only, as the distributions carried out with Mode 3 vs. Mode 4 led to similar observations).

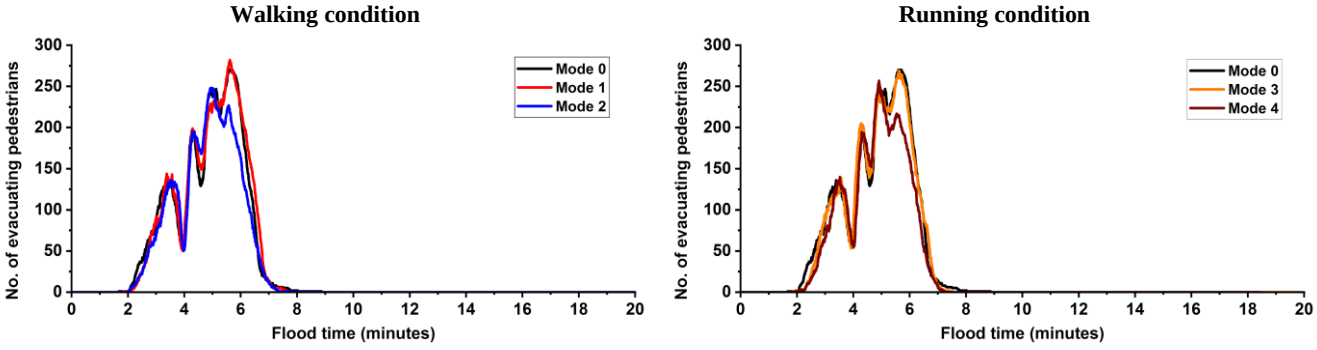

(a) Evacuating pedestrians with a toppling-only condition

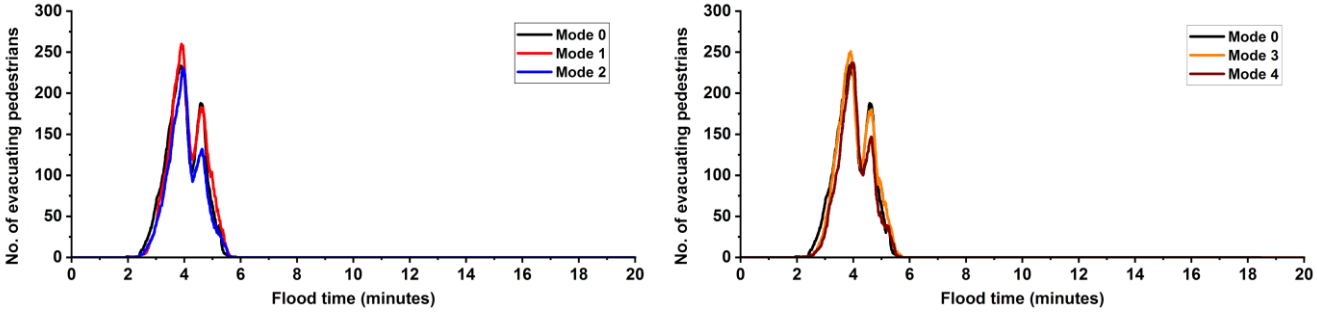

(b) Evacuating pedestrians with a toppling-and-sliding condition

Figure 5: Number of evacuating pedestrians with stability state predicted by the simulator under Mode 0 (baseline outcomes from the previous version of the simulator (Shirvani et al., 2020); Mode 1 or Mode 2 (age-related walking condition for the moving speeds without or with the two-way interaction condition); and Mode 3 or Mode 4 (age-related running condition for the moving speeds without or with the two-way interaction condition). Sub-figures (a) and (b) include the stability states with a toppling-only condition and a toppling-and-sliding condition, respectively, when immobilised in floodwater

Figure 6 overlaps the spatial distributions of the evacuating pedestrians and the flood HR map at two critical times of the flooding, 3.6 min and 4.6 min. The circled areas indicate higher-than-medium risk zones of floodwater flow with HR > 1.5. As shown in Fig. 6a, at 3.6 min, the two-way interaction condition magnifies the higher-than medium risk zones at the tail of the crowding leading to more pedestrians at risk of being in a toppling-only or a toppling-and-sliding conditions. Whereas, at 4.6 min (Fig. 6b), the two-way interaction condition led to having less pedestrians with a toppling-and-sliding condition in the heart of the crowded area, where their stability state changed to a toppling-and-sliding condition.

https://doi.org/10.5194/nhess-2021-79
Preprint. Discussion started: 23 March 2021

Natural Hazards and Earth System Sciences
Discussions

In terms of total time to evacuate the 1,000 pedestrians, the simulator predicted around 13 min with Mode 0, 18 min with Mode 1, 19 min with Mode 2, 11.7 min with Mode 3 and 11.5 min with Mode 4. Contrasting the predicted times reinforces previous findings from Fig. 4: compared to Mode 0, the age-related walking speeds (Mode 1) predicts a slower evacuation time and enabling it with the two-way condition (Mode 2) increases slightly the evacuation time as crowding is more likely under the walking condition. The age-related running speeds (Mode 3) leads to a shorter evacuation time than with the other modes, that are slightly reduced when enabling the two-way condition (Mode 4). Next, the simulator is only run under Mode 2 to analyse a mass evacuation of pedestrians that mostly have low to medium flood risk states (Sect. 3).

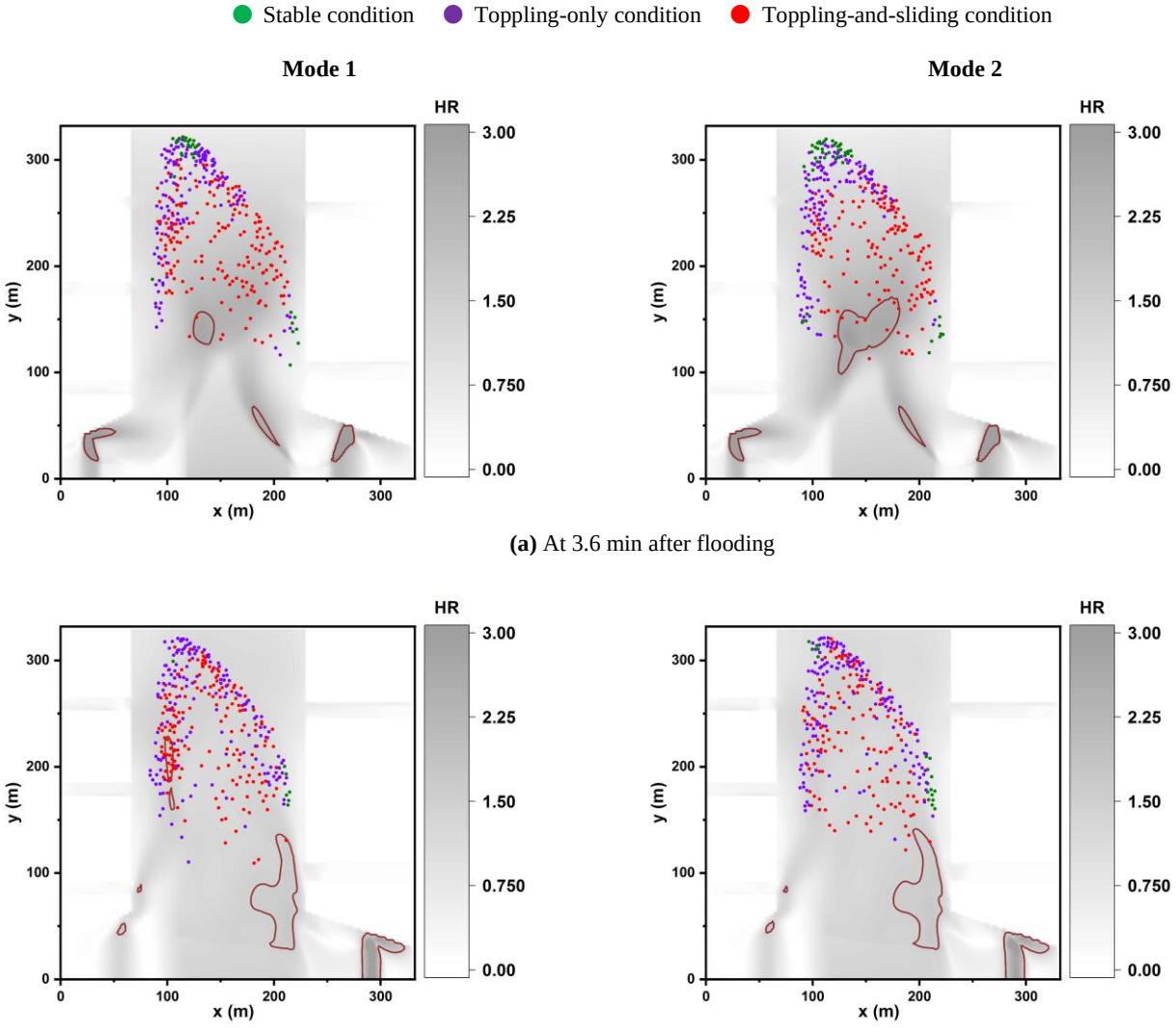

(a) At 3.6 min after flooding

(b) At 4.6 min after flooding

Figure 6: Spatial distribution of pedestrian agents, represented by coloured dots, predicted by the simulator under Mode 1 (left panel) and Mode 2 (right panel) at two different flood times: (a) 3.6 min after flooding and (b) 4.6 min after flooding. The grey colour represents the

https://doi.org/10.5194/nhess-2021-79
Preprint. Discussion started: 23 March 2021

Natural Hazards and Earth System Sciences
Discussions

floodwater extent based on the flood HR quantity and the red-circled areas show where the HR is greater than 1.5, indicative of a high-to-highest flood risk.

3 Real-world case study

3.1 Background and scenario description

The case study consists of a site located outside of the main entrance of Hillsborough football stadium in Sheffield. The location of the site is framed with a red square in Fig. 7, including an area of 16,384 m^2 that is adjacent to the eastern side of the stadium, where the main entrances/exits are located (yellow line in Fig. 7). The stadium entrances are opened to a T-junction streetscape that constitutes the walkable area including all the main roads and pedestrian pathways (this area is framed in Fig. 7). The main roads are open from the south, east and north sides of the walkable area (shown with the green lines), and these openings are likely to constitute the most popular destinations where spectators would go before and after a football match.

Figure 7: The study site (red square) including the walkable area (red area within the red square) where people normally use to go to their different destinations located in the south, east and north sides of the walkable area (green lines) after they leave the stadium from the main entrances (yellow line), © Google

The stadium can accommodate up to 39,732 spectators, and usually has an average attendance rate of around 24,000 per each home football match in normal weather conditions (Football Web Pages: Sheffield Wednesday, available at: www.footballwebpages.co.uk/sheffield-wednesday). This site would therefore be occupied by large numbers of pedestrians, including football fans before and after a match, even in the aftermath of a flood as, for example, happened for the November 2019 Sheffield floods (Pugh, 2019). This site also experienced flooding in the 2007 UK floods, due to extreme rainfall, of around 100 mm in one day (Environment Agency, 2007). The historical 2007 flood suggests that rainfall runoff would cause floodwater inundation to spread along the northern side of the stadium, and to accumulate within the selected site where it

https://doi.org/10.5194/nhess-2021-79
Preprint. Discussion started: 23 March 2021

submerged pedestrian pathways, parking lots and the stadium pitch. Worries of a similar event were expressed during the 2019 Sheffield floods that were caused by seven-day continuous rainfall of 63.8 mm. This led to a cancelation of a football match as water level slightly overtopped the flood defence protecting the stadium from the River Don. The event, if happened during the football match, could put many in and around the stadium at a high risk.

Being both adjacent to River Don and located down the hills where rainwater runoff accumulate, this site has been flagged to be prone to future pluvial or fluvial flooding types according to EA's online flood maps for planning (available online at: https://flood-warning-information.service.gov.uk/long-term-flood-risk). Figure 8 shows a screenshot of the EA's floodwater depth map for the walkable area covering the cases of 'low', 'medium' and 'high' annual flooding probabilities. Even though with the 'low' flooding probability scenario, floodwater inundation would still reach a depth of 0.9 m, which is high enough to force people to select unusual pathways or temporarily change their direction towards another destination to avoid the floodwater as they evacuate.

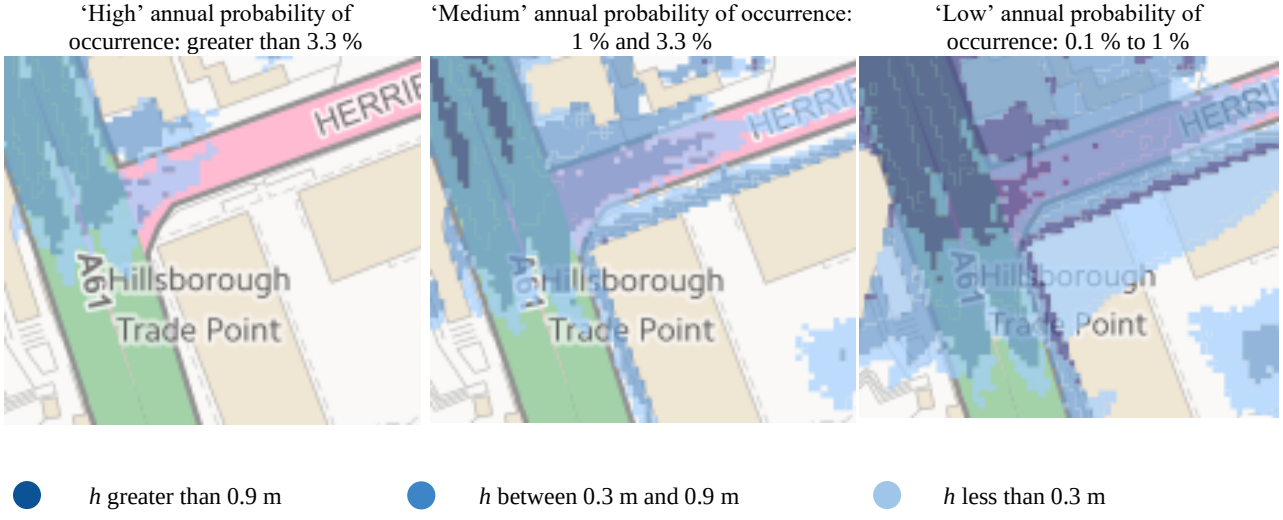

Figure 8: Screenshots showing the floodwater depth map for the walkable area covering the cases of 'low', 'medium' and 'high' annual flooding probabilities. These screenshots were retrieved from https://flood-warning-information.service.gov.uk/long-term-flood-risk (credit: © Crown and database rights under Open Government Licence v3.0).

In this study, it is assumed that the site in Fig. 7 is hit by a flood, similar to the one that had happened in 2019, during a football match where the spectators are caught unaware of the rainfall accumulation around the stadium. The floodwater occurs from the north-east side and moves and accumulates downhill towards the main entrance of the stadium. Once the floodwater approaches the main entrances, an emergency evacuation alarm is issued urging people to evacuate the stadium immediately. The spectators are then put into queues inside the stadium, waiting to be evacuated towards the walkable area. The evacuated spectators gradually enter the walkable area where they get in direct contact with the propagating floodwater along their ways to any of the south, east or north destinations. The walkable area was measured to have a size of 8,161 m^2, and a reduced

https://doi.org/10.5194/nhess-2021-79
Preprint. Discussion started: 23 March 2021


Natural Hazards and Earth System Sciences Discussions

number of 4,080 spectators (2 person per square metre) are assumed to have attended the football match, given the extreme weather conditions. This population size respects the highest safety limit for moving and queueing states at sports grounds (Still, 2019). Using a bigger population size would lead to extreme pedestrian congestion that impacts the movements of individual pedestrians, governed by the social force model (Minegishi and Takeichi, 2018). Hence, limiting the number to 4,080 pedestrians is also helpful to more realistically evaluate the net effect of pedestrian behaviours in relation to the changes in the state of floodwater variables during the evacuation process.

The flood-pedestrian simulator is applied to simulate this scenario for analysing the pedestrian evacuation patterns including their preference for the destination during flood evacuation, by activating the 'autonomous change of direction' condition (Sect. 2.2.3).

3.2 Simulator configuration

To simulate the evacuation scenario, the simulator was gradually configured; first, using its hydrodynamic model alone to ensure that it replicates the floodwater hydrodynamic upon a realistic terrain and driven by a hydrograph representing the extreme rainfall event that occurred in November 2019 (Sect. 3.2.1); and, then, by further configuring its pedestrian model with scenario-specific characteristics for the pedestrian agents considering population age, gender, height, probability of destination selection, and thresholds of floodwater depth to body height required for the 'autonomous change of direction' condition (Sect. 3.2.2).

3.2.1 Hydrodynamic model set-up

The hydrodynamic model was set up to run on a grid of 128 × 128 flood agents. The grid of flood agents (equally for the grid of navigation agents) was set to store the terrain features of the study site, loaded from a digital elevation model (DEM) at 1 m resolution, which is available online from the UK's Department for Environment Food & Rural Affairs (DEFRA) LiDAR Survey (available at: https://environment.data.gov.uk).

To generate the flood propagation from the north-east side of the site, an inflow hydrograph (Fig. 9) was generated based on the November 2019's rainfall data. The hydrograph was set to replicate a total runoff volume accumulation of 1,045.3 m^3 based on a 0.0638 m rainfall over the entire 16,384 m^2 site. This volume was estimated using the direct runoff method: *rainfall volume* (m^3) = *rainfall height* (m) × *area* (m^2). The hydrograph was generated as:

$$Q_t = Q_{initial} + (Q_{peak} - Q_{initial})(\frac{t}{t_{peak}}.exp(\frac{1-t}{t_{peak}}))^{\beta}, \quad (3)$$

where Q_t (m^3/s) is the inflow discharge propagating along the north-east boundary intersecting with the road; Q_{peak} (m^2/s) = 0.29 is the peak discharge, that was calculated by distributing the runoff volume (1,045.3 m^3) per second over an hour of flooding; $Q_{initial}$ (m^3/s) is the initial discharge, taken 0 m^3/s; t (min) is the simulation time varying between 0 to 10 min; β = 10 is a constant to soften the shape of the hydrograph and t_{peak} (min) = 5 is the time of peak discharge. This choice, for t_{peak},

https://doi.org/10.5194/nhess-2021-79
Preprint. Discussion started: 23 March 2021

Natural Hazards and Earth System Sciences
Discussions

considers the peak discharge has been reached halfway during the flooding to cause the propagating floodwater to reach to the main stadium's entrances by 10 min leading to triggering the evacuation alarm.

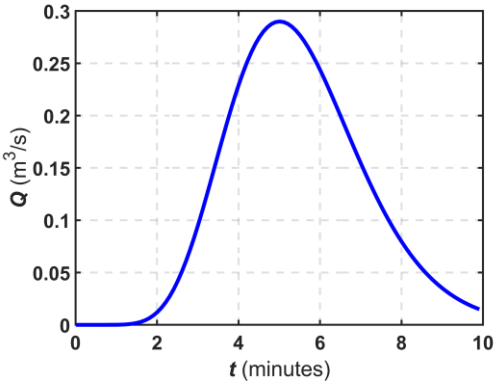

Figure 9: Inflow hydrograph produced by Eq. (3) used to generate the floodwater propagation occurring from the north-east side of the site

To evaluate whether the floodwater resulting from the hydrograph would resemble reality, the simulator was run, without pedestrian consideration, to analyse the extent to which the predicted range for the floodwater depth (Fig. 9) agrees with that predicted by in the EA's flood risk maps (Fig. 8). At the end of simulation (t = 10 min), the states of floodwater variables stored by all the flood agents were extracted. The information relevant to the depth of floodwater was used to plot a flood map that is shown in Fig. 10a. The flood map in Fig. 10a suggests a maximum water level of 0.9 m over the walkable area and that the highest and lowest risk zones are located in the north-west and south, respectively, thus in good agreement with the risk extents and range of floodwater depths reported by the EA's (Fig. 8). The information of the states of the floodwater variables were also analysed for the HR flood map to gain an insight into the potential flood risk states that pedestrians would be having within the walkable area. Fig. 10b shows the HR flood map at 10 min, all over which the HR reaches a maximum value that is slightly greater than 1.5, suggesting that the majority of pedestrians would be having low to medium flood risk states at the onset of evacuation. Overall, the generated inflow hydrograph is able to replicate realistic floodwater depths and extents within the walkable area where the majority of pedestrians would be expected to mostly be at a low to medium flood risk state. Next, the simulator is applied with pedestrian considerations while re-running the hydrodynamic model with a lag of 10 min in the simulation time, t = - 10 min, to account for the fact that the evacuation started at t = 0 min (so enough time had passed for the floodwater to partially submerge the highest risk zones in the site).

https://doi.org/10.5194/nhess-2021-79
Preprint. Discussion started: 23 March 2021

Natural Hazards and Earth System Sciences
Discussions

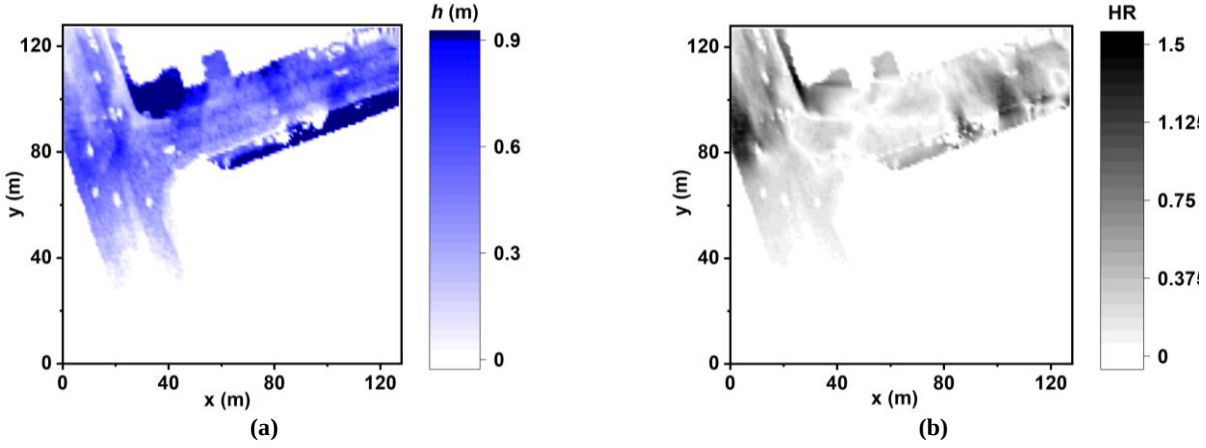

Figure 10: Flood maps generated after 10 min of a single hydrodynamic without pedestrian consideration run based on: (a) floodwater depth and (b) HR extent over the entire site

3.2.2 Pedestrian model set-up

The pedestrian model was also set up for a grid of 128 × 128 navigation agents encoding the topographic features of the site, i.e. the boundaries, location of exits/entrances, and obstacles, into the navigation map. Hence, the navigation map has also a resolution of 1 m over which the pedestrian agents receive information about their destinations. The pedestrian model was set to gradually generate 4,080 pedestrian agents with a rate of 4 pedestrian agents per second starting at simulation time t = 0 min, to ensure safe evacuation timing for crowd evacuation planning in stadiums (Minegishi and Takeichi, 2018). Once a pedestrian agent is generated, it is assigned a random (initial) destination, to which they start to move to, between the three available destinations with an equal probability (south, east or north shown in Fig. 7). Along their ways, each pedestrian agent receives information on the state of floodwater variables, via the navigation agent at their specific time and location, based on which it makes a decision on whether to alter their direction to another destination.

As the case study consists of an outdoor urban environment with no specific destination, the pedestrian agents are set to dynamically alter their destination by activating the 'autonomous change of direction' condition (Sect. 2.2.3). This condition allows pedestrian agents to auto-select new pathways after processing the received information on the state of the floodwater variables. As explained in Sect. 2.2.3, this condition requires specifying a threshold of floodwater depth to body height beyond which a pedestrian agent considers shifting their walking direction and looking for a new destination within 100 seconds. After this period, if the pedestrian agent remains undecided, it is set to pick the destination selected by the majority of its neighbouring pedestrian agents, on the basis that it was influenced by the choice of others around (Sect. 2.2.3).

As people may underestimate the floodwater risk and can enter floodwater from different risk perceptions (Becker et al., 2015; Netzel et al., 2021), three thresholds of floodwater depth to body height were investigated to accommodate this uncertainty (Fig. 11). The '20 % threshold' was defined to represent people with high-risk perception, who may not enter floodwater with a depth that is more than 20 % of their body height. This threshold, for this case study, is estimated based on

https://doi.org/10.5194/nhess-2021-79
Preprint. Discussion started: 23 March 2021

Natural Hazards and Earth System Sciences
Discussions

the ratio of the dominant minimum value for the depth of floodwater that can occur over the walkable area (0.3 m) to the height of the shortest pedestrian agent available (1.4 m). With this threshold, the likelihood of the entire population to be in a condition to change their direction is ensured. The '40 % threshold' was defined to represent people with low-risk perception, who may enter a floodwater with a depth that is even more than 40 % of their body height. This threshold, for this case study, is estimated based on the ratio of the dominant maximum depth of floodwater (0.9 m) to the height of the tallest population of pedestrian agents available (2.1 m). This threshold enables the entire population to have the freedom to keep moving even within the deepest floodwater in the walkable area (0.9 m). The '30 % threshold' was defined based on an average-risk perception, and is selected as it represents the knee height of humans, irrespective of their body height (Teichtahl et al., 2012).

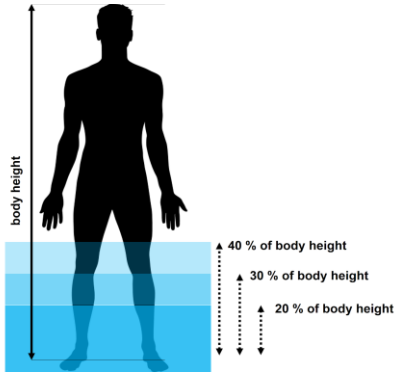

Figure 11: Thresholds of floodwater depth to body height that are specified for pedestrian agent to accommodate uncertainty associated with different risk perception of people in the real-world case study

The characteristics of pedestrian agents were adapted to consider the age, gender and height distribution of football fans in the UK. Therefore, the randomised age distribution reported in Sect. 2.2.1 was increased by 5 %, 8 % and 4 % for the age groups of 30 to 39, 40 to 49, and 50 to 59 in order to replicate the higher attendance of these age groups to live sports events in England (Lange, 2020). Also, the randomised gender distribution was changed to 67 % males and 33 % females based on a survey on the gender distribution of football fans in the UK (Statista Research Department, 2016). In terms of body height, the pedestrian agents were based on the same UK body height distribution used previously (Shirvani et al., 2020).

3.2.3 Simulation runs

The simulator was run under configuration Mode 2, which was deemed suited for the scope of this case study (Sect. 2.3.2). Three simulations were performed by considering each of the 20 %, 30 % and 40 % thresholds in the 'autonomous change of direction' condition, respectively (visualisation of the simulations can be found in the video supplement in Shirvani (2021)). Outputs from each simulation run included spatial and temporal information, at each time step, about the pedestrian agents as they evacuate (t > 0 min). The predicted outputs include the position, flood risk state (HR-related), stability state (with a toppling-only condition and a toppling-and-sliding condition), and the choice for the destination selected by the pedestrian agents during the evacuation process. These outputs are analysed for each the 20 %, 30 % and 40 % thresholds, considering

https://doi.org/10.5194/nhess-2021-79
Preprint. Discussion started: 23 March 2021


Natural Hazards and Earth System Sciences Discussions

585 the popularity of the destination selected by the pedestrian agents (among south, east and north) together with their flood risk
586 state and stability state.

587 **3.3 Analysis of the results**

588 Figure 12 shows the total number of evacuating pedestrians in the walkable area, plotted according to the pedestrians' choices
589 among the three destinations located to the south, east and north of the stadium, for the 20 %, 30 % and 40 % thresholds. All
590 the simulated evacuation patterns show a decrease in the total number of pedestrians after 22 min of flooding. This suggests
591 that 22 min would be required for the 4,080 pedestrians to vacate the stadium, and that the choice for the threshold does not
592 have any effect on the density of pedestrians evacuating.

593 The simulated evacuation patterns obtained with the 20 % threshold are shown in Fig. 12a, suggesting that most of
594 the pedestrians evacuated the walkable area within 35 min. The majority of the evacuating pedestrians start favouring the south
595 destination after 5 min, indicating that after this time the floodwater depth is beyond 20 % of their body height over the
596 pathways of the walkable area extending towards the east and north destinations. After 5 min, the south destination remained
597 the most popular destination, selected by more than 55 % of the pedestrians; whereas, the east and north destinations were less
598 popular, selected by 25 % and 20 % of the pedestrians, respectively.

599 With the simulated evacuation patterns obtained with the 30 % threshold (Fig. 12b), a longer evacuation time is
600 predicted for the majority of the evacuating pedestrians. Now it takes about 45 min for most of the pedestrians to leave the
601 walkable area and the popularity of the east and north destinations increased, with slightly more evacuating pedestrians
602 preferring them, about 25 % and 25 %, respectively. This suggests that 5 % more of the pedestrians considered changing their
603 destination to the north where the floodwater depth can only reach up to their knee height. Still, as with the 20 % threshold,
604 the south destination was the most popular and started to favour after 5 min by 50 % of the pedestrians.

605 With the simulated evacuation patterns obtained with the 40 % threshold (Fig. 12c), a significant change in the
606 favoured destination is observed alongside an even more prolonged evacuation time. Now, it takes about 55 min for most of
607 the pedestrians to evacuate the walkable area and the popularity of the south destination decreased significantly, compared to
608 the predicted evacuation patterns obtained with the lower thresholds. Here, the south destination was only picked up by 25 %
609 of the pedestrians and the north destination was preferred instead (by around 50 % of the evacuating pedestrians) since the
610 very beginning of the evacuation. As for the east destination, it remained equally popular as with evacuation patterns obtained
611 with the lower thresholds, and was selected by around 20 % of the evacuating pedestrians.

612 The simulated evacuation patterns in Fig. 12 imply that the south destination would be the preferred by people who
613 are less likely to enter floodwater with a depth beyond their knee height, and that the north destination would be preferred by
614 those willing to enter the deeper floodwater. The results also suggest longer evacuation times when people are willing to enter
615 the floodwater at a depth beyond their knee height.
616

https://doi.org/10.5194/nhess-2021-79
Preprint. Discussion started: 23 March 2021

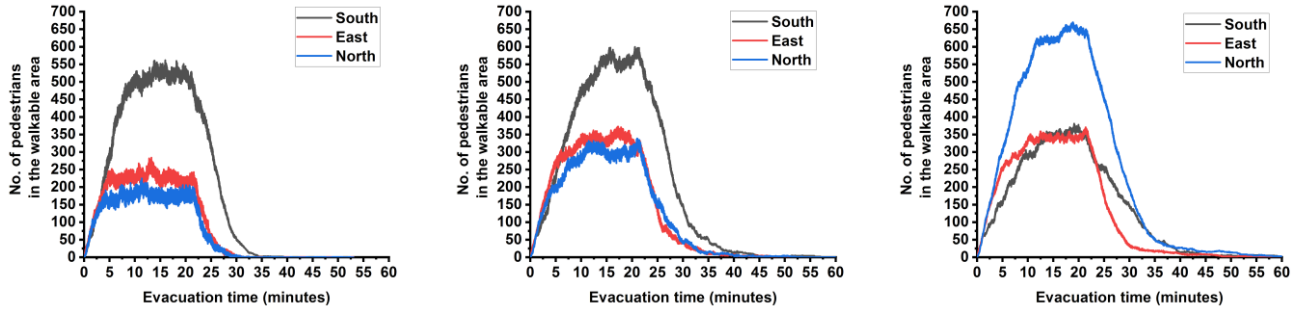

(a) 20 % threshold **(b)** 30 % threshold **(c)** 40 % threshold

Figure 12: Total number of evacuating pedestrians in the walkable area plotted according to their destination choices for the south, east and north during the evacuation time: (a) 20 % threshold, (b) 30 % threshold and (c) 40 % threshold

The flood risk states and stability states with toppling-only or toppling-and-sliding conditions for the pedestrians are shown in Fig. 13 for the three simulations obtained with the 20 %, 30 % and 40 % thresholds. Fig. 13-left includes the flood risk states as well as the total number of evacuating pedestrians in the walkable area. As the threshold increased, the total number of pedestrians in the walkable area is seen to increase, leading to prolonged evacuation times. This observation is aligned with that made for Fig. 12, suggesting that the evacuation process would be delayed as more evacuating pedestrians enter the deeper floodwater where their moving speed reduces. The number of pedestrians in dry zones remains constant, despite the choice for the threshold. This may be expected as these pedestrians represent those who had initially decided to go towards the south destination (one third of the pedestrians) and did not find a need to alter their destination during the process given the dominance of dry areas within south parts of the walkable area (see Fig. 10). For the three thresholds, the majority of the evacuating pedestrians were found to be at a low flood risk state (HR < 0.75). Up to around 20, 100 and 200 evacuating pedestrians reached a medium flood risk state (0.75 < HR < 1.5) with the 20 %, 30 % and 40 % thresholds, respectively. Up to only 15 pedestrians had a high risk flood state (HR > 1.5) and this only occurred for those who entered the floodwater at a depth beyond 40 % of their body height.

The number of evacuating pedestrians that could have a stability state with a toppling-only or toppling-and-sliding conditions are shown in Fig. 13-right. For the 20 % threshold, very few pedestrians were found to have these stability states, up to 15 in number. Findings in Shirvani et al. (2020) suggest that these could be pedestrians with a low flood risk state (HR < 0.75) with a toppling-only condition or with a medium flood risk state (0.75 < HR < 1.5) with a toppling-and-sliding condition. The number of pedestrians with these conditions for the stability states increased with the threshold of 30 %, which is expected given the increased number of pedestrians under a low and medium flood risk state evacuating over a longer period. Up to 60 and 30 more pedestrians were found to be with toppling-only and toppling-and-sliding conditions, respectively. With the 40 % threshold, 20 more pedestrians were found to be with a toppling-and-sliding condition, and up to 200 more were found to be with a toppling-only condition. The significant increase in the number of pedestrians with a topping-only condition

https://doi.org/10.5194/nhess-2021-79
Preprint. Discussion started: 23 March 2021

Natural Hazards and Earth System Sciences
Discussions

642 is expected with the 40 % threshold, for which more pedestrians would be entering the floodwater where its depth is beyond
643 their knee height.

644 The analysis of the flood risk and stability states suggests that the majority of people evacuating the stadium would
645 take an evacuation route that is either dry or keeps them under a low flood risk state (HR < 0.75) with a toppling-only condition
646 during the evacuation. Less people would be entering deeper floodwater and, when they do, they are expected to be in a
647 medium flood risk state (0.75 < HR < 1.5) where they can have a toppling-and-sliding condition.
648

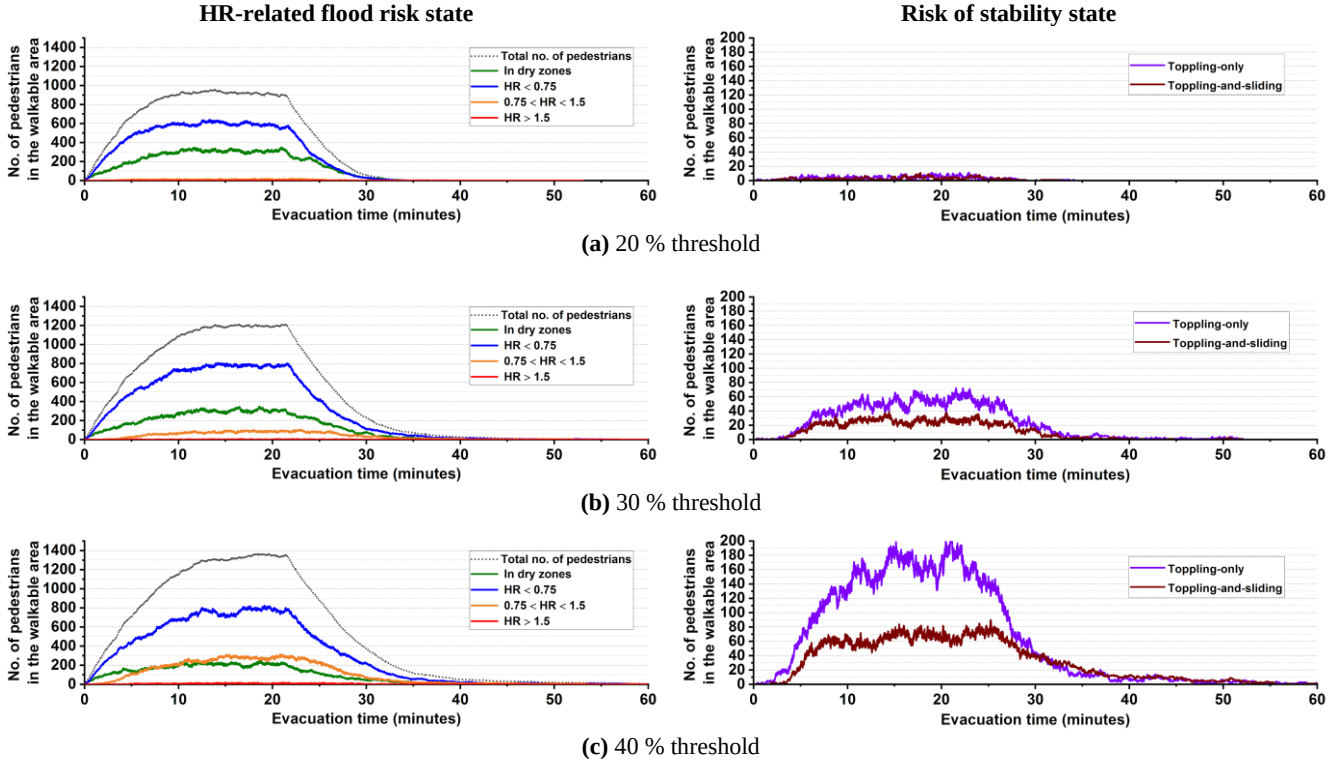

(a) 20 % threshold

(b) 30 % threshold

(c) 40 % threshold

649 **Figure 13:** Total number of evacuating pedestrians in the walkable area plotted according to their HR-related flood risk state (left panel)
650 and stability state when they were immobilised in floodwater (right panel) during the evacuation time: (a) 20 % threshold, (b) 30 % threshold
651 and (c) 40 % threshold

652 Figure 14 shows the 2D spatial distribution of the evacuating pedestrians over the HR flood map at 22 min when
653 pedestrian presence in the walkable area is at its highest as soon as everyone vacated the stadium. The pedestrians are
654 represented by dots with different colours representing their stability state based on the predictions made with the 20 %, 30 %
655 and 40 % thresholds. The evacuation patterns in Figure 14, though retrieve many of observations made before (through Fig.
656 12 and Fig. 13) demonstrate the simulator's further ability to inform on the potential locations where the evacuating pedestrians
657 are expected to be immobilised by the floodwater. With the 20% threshold (Fig. 14a), most of the pedestrians remained mobile
658 in the floodwater (stable condition) and preferred the south destination where low flood HR dominates. From the remaining
659 pedestrians, who preferred the east or north destinations, a handful were immobilised by floodwater (toppling-only or toppling-

https://doi.org/10.5194/nhess-2021-79
Preprint. Discussion started: 23 March 2021

Natural Hazards and Earth System Sciences
Discussions

and-sliding conditions). These states of immobility are observed to occur at two vicinities where the flood HR varied from the upper low range to the medium range: within the north-east pathways located at the streets' intersection leading to the north destination, and within middle of the eastern the pathways leading to the east destination. The spatial distributions predicted with the 30% threshold (Fig. 14b) also suggest a preference for the south destination by most of the pedestrians, and that many more pedestrians would be immobilised by the floodwater within the aforementioned vicinities. There, at least a dozen would have a stability state with a toppling-and-sliding condition caused by the relatively higher number of pedestrians who kept moving to the north and east destinations. With the 40% threshold (Fig. 14c), most of the pedestrians were still found to be mobile in floodwater (stable condition) despite the fact that the (riskiest) north destination was the dominant choice. However, the spatial distributions predicted with this threshold point to a major increase in the number of immobilised pedestrians within the aforementioned vicinities.

The analysis in Fig. 14 suggests that people who avoid entering a floodwater depth beyond their knee height are most likely to select the south destination, where their condition remains stable to keep evacuating with minimum risk of immobilisation. Those with a tendency to enter deeper floodwater would go to the east or north destinations, towards which the majority would still be able to evacuate, but at a slower pace delayed by the risk of facing immobilisation as they move forward to their selected destination. Overall, the predictions produced by the simulator (Fig. 12 to Fig. 14) seem sensible, suggesting that it can be a useful tool for planning people evacuation scenarios in small urban areas to a flood emergency.

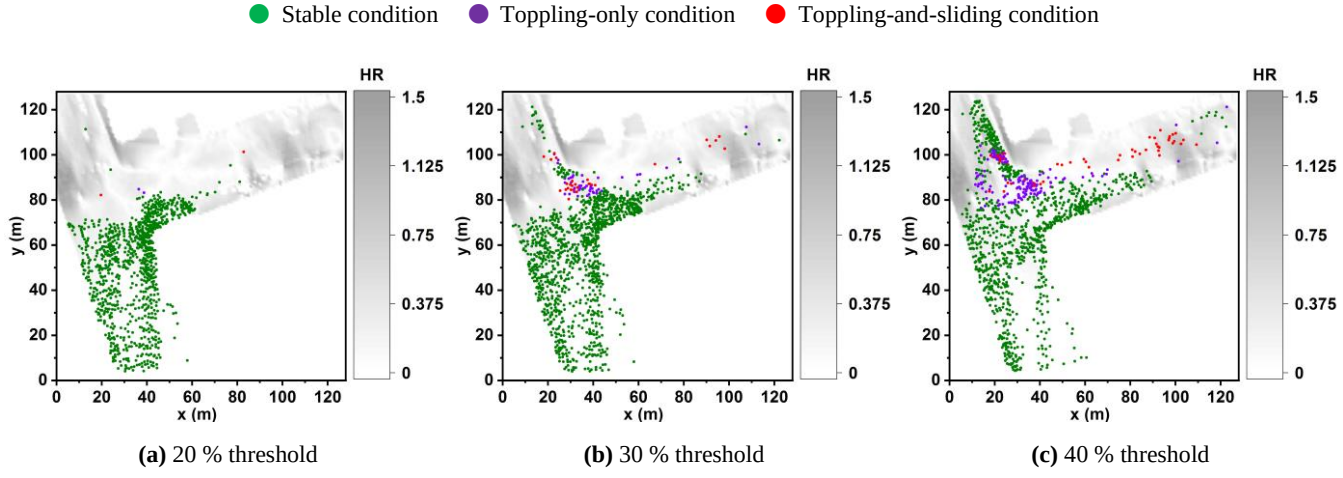

(a) 20 % threshold **(b)** 30 % threshold **(c)** 40 % threshold

Figure 14: The spatial distribution of pedestrians over the walkable area under the predicted stability states (coloured dots) along with the HR flood map (grey shade) at simulation time t = 22 min, when the number of pedestrians over the walkable area is at highest after all of them had vacated the stadium: (a) 20 % threshold, (b) 30 % threshold and (c) 40 % threshold

https://doi.org/10.5194/nhess-2021-79
Preprint. Discussion started: 23 March 2021


Natural Hazards and Earth System Sciences Discussions

4 Summary, discussions and limitations

The flood-pedestrian simulator was augmented to more realistically model the dynamics of pedestrian responses around and inside urban floodwaters. The simulator couples a hydrodynamic model to a pedestrian model in a single agent-based modelling platform which allows dynamic exchange and processing of data between the two models as they update in time. The hydrodynamic model is built upon a fixed grid of discrete 'flood' agents, storing and updating information of floodwater in space and time. The pedestrian model also involves a fixed grid of discrete 'navigation' agents that encodes the (urban) features of the walkable area over which continuous type 'pedestrian' agents move in space and time as they interact with each other and make way-finding decisions. The grids of navigation and flood agents are overlapped, allowing the navigation agents to dynamically receive hydrodynamic information to further inform pedestrian agents' way-finding decisions when they move in the floodwater. The pedestrian agents were featured with realistic human body characteristics and in-model behavioural rules based on which their flood risk states, stability states, moving speeds and way-finding decisions are defined at their certain location and output time. The flood risk states were defined using the flood HR quantity, expressed in terms the floodwater depth and velocity magnitude, to be either low, medium, high or highest (Table 1). Experimentally derived formulas were used to define individual stability states based on analysing the floodwater depth and velocity magnitude and specific body height and mass of the pedestrian agents. These states include a stable condition of mobility in the floodwater or immobilisation conditions from toppling-only or toppling-and-sliding (Table 2). The stability states in the present simulator were defined based on more realistic body mass and height that are age and gender related (Table 3). This version of the simulator is also featured by a set of more realistic moving speeds defining the mobility of the pedestrian agents around and inside the floodwater: the social force model was adapted to consider empirically based age- and gender-related walking speeds in dry zones and a maximum excitement condition inducing faster walking speeds around the floodwater (Table 4); and, when inside the floodwater, experimentally derived moving speeds were applied with either a walking condition or a running condition (Table 5). The walking and running conditions can be applied without and with a two-way interaction condition that considers the effects that pedestrian congestion may have on the floodwater dynamics, and vice versa. A new autonomous change of direction condition was added to make the way-finding decisions of pedestrian agents become self-automated (Sect. 2.2.3), informed by the state of the floodwater dynamics or the choices of pathways selected by their neighbouring agents. This condition required introducing a threshold of a floodwater depth to body height beyond which a pedestrian agent decides to change direction and a waiting time after which the pedestrian agent is assigned the most popular pathway selected by the others around.

The conditions factoring in the added characteristics and in-model behavioural rules were evaluated for a test case of a flood evacuation in a shopping centre. This indoor evacuation test case was selected as it was investigated with the previous version of the simulator with which the mobility and stability states of the pedestrian agents were driven by rules without considering age and gender influences, thus allowing to evaluate the added rules and characteristics. The evaluation procedure was based on systematically enabling any of the new age- and gender-related conditions (Table 6), and analysing the changes

https://doi.org/10.5194/nhess-2021-79
Preprint. Discussion started: 23 March 2021


Natural Hazards and Earth System Sciences Discussions

they induce in the simulated pedestrian evacuation patterns with reference to the baseline patterns obtained from the previous version of the simulator. The analysis of the simulated pedestrian evacuation patterns indicate major differences with the baseline evacuation patterns using any of the new conditions. Using the walking condition, the simulator predicted much more pedestrians with a low flood risk state exhibiting slower evacuation patterns, and less pedestrians with a medium flood risk state exhibiting faster evacuation patterns before reaching the highest density of the crowd in the walkable area. With the running condition, no major changes in the evacuation patterns were observed compared to those predicted with the walking condition for the pedestrians with a medium flood risk state; however, those with a low flood risk state were predicted to have relatively faster evacuation patterns, even compared to the baseline predictions. With either of the running or walking conditions, only few pedestrians were predicted to be evacuating in a high risk state, which is in contrast with the baseline patterns indicating much more pedestrians to be evacuating. Fewer pedestrians were predicted to be evacuating with the highest risk state, as was also the case with the baseline predictions; however, using either of the running or walking conditions predicted earlier times of highest risk exposure. Choosing either of the running or walking conditions with the two-way interaction condition was noted to accelerate the evacuation patterns for the pedestrians with a low to medium flood risk state. This was particularly observed at flooding time after reaching the highest density of the crowd in the walkable area, leading to more significant reduction in the floodwater hydrodynamics and, in turn, reduction of the state of immobility for many of the pedestrians with a low to medium risk state. Overall, the new features led to different evacuation patterns than the baseline patterns. With the walking condition, the simulator is expected to only lead to major differences in the evacuation patterns of pedestrians in a low flood risk state. This condition is a sensible choice when applying the simulator to study a mass evacuation together with the two-way interaction condition, which could significantly affect the evacuation patterns when there is crowding of pedestrians in low to medium flood risk state.

The utility of the simulator, with the new autonomous change of direction condition, was then demonstrated over a real-world case study of a mass evacuation of football spectators attending a match into a T-junction streetscape, in response to a flood emergency. The study site included the streetscape and the entrance of Hillsborough football stadium in Sheffield, and is prone to flooding that would expose pedestrians to low-to-medium flood risk states. The streetscape leads to three ends, towards the north, east and south, any of which could be a designation for pedestrians. The simulator was set up to replicate historical extents and depths of the floodwater that would inundate this study site, to consider the age- and gender-characteristics of football spectators, and by enabling the walking condition together with the two-way interaction condition. The autonomous change of direction condition was applied based on three thresholds of a floodwater depth to body height: 20% threshold, 30% threshold and 40% threshold, representative of a high, medium and low level of people's risk perception. The simulated evacuation patterns suggest that when people exhibit high to medium risk perception, avoid zones of floodwater depth beyond their knee height, the majority change direction to go to the south destination that has the highest portion of dry zones. Whereas, when people exhibit a low risk perception, enter zones of floodwater depth slightly higher than their knee height, the majority would take the shallowest pathway leading to the north destination. As the risk perception level decreased, the simulated evacuation patterns showed an increase in the number of people in a medium risk state with an immobilised

https://doi.org/10.5194/nhess-2021-79
Preprint. Discussion started: 23 March 2021


Natural Hazards and Earth System Sciences Discussions

condition and longer evacuation time. The investigations over the real-world case study demonstrates that the flood-pedestrian simulator can be usefully used to analyse the dynamics of people's responses in and around the floodwater as part of the flood risk analysis, thus is a useful tool for planning evacuation of crowds to flood emergencies in small and potentially congested urban areas.

However, the flood-pedestrian simulator has a number of considerations and limitations that are worth mentioning. Firstly, the simulator requires the accessibility to a Graphical Processing Unit (GPU) card and the generation of input files requires special .xml translation specific to FLAMEGPU and using the FGPUGridNavPlanEditor toolkit (available at: https://github.com/RSE-Sheffield/FGPUGridNavPlanEditor). Secondly, the simulator can provide a live visualisation showing hydrodynamic and pedestrian information changing in real time, when run on windows using the console mode (Shirvani, 2021). Thirdly, in terms of pedestrian characteristics, the simulator does not incorporate the uncertainties associated with social and psychological characteristics of people, e.g. flood tourism, as well as their floating and sinking conditions. Lastly, but not least, the assumptions and thresholds used to implement the two-way interaction condition and the autonomous change of direction condition are both lacking any existing empirical evidence base supported by dedicated laboratory experiments.

Code availability

The flood-pedestrian simulator is accessible from Zenodo open-access repository at https://doi.org/10.5281/zenodo.4564288, with a link to the GitHub source codes of the latest release, including a detailed 'run guide' and input files to enable the users to run the flooded shopping centre and the Hillsborough stadium evacuation test cases on their own machine. The previous version of the simulator is also available on DAFNI, available at: https://dafni.ac.uk/project/flood-people-simulator/, where it can be run from a user-friendly graphical interface and supported by a run guide.

Data availability

Outputs of the simulations are available in the Zenodo open-access repository at https://doi.org/10.5281/zenodo.4576906.

Video supplement

Demo videos of the test cases are available online in the TIB AV-Portal at https://doi.org/10.5446/51547.

Author contribution

MS contributed to developing the simulator, design of the test cases, running simulations, obtaining outputs and figure preparation. GK proposed the research approach and supervised the development, testing, scenario configurations and analysis

of the outputs, and obtained the research grant. MS and GK prepared the manuscript. All authors read and approved the final paper.

Competing interests

The authors declare that they have no conflict of interest.

Acknowledgements

This work is part of the SEAMLESS-WAVE project (SoftwarE infrAstructure forMulti-purpose fLood modElling at variouS scaleS based on WAVElets), which is funded by the UK Engineering and Physical Sciences Research Council (EPSRC) grant EP/R007349/1. For information about the SEAMLESS-WAVE project visit https://www.seamlesswave.com. The authors wish to thank Paul Richmond and the Research Software Engineering (https://rse.shef.ac.uk/) group for providing technical support during the implementation of the flood-pedestrian simulator on FLAMEGPU.

References

Abebe, Y.A., Ghorbani, A., Nikolic, I., Manojlovic, N., Gruhn, A. and Vojinovic, Z.: The role of household adaptation measures in reducing vulnerability to flooding: a coupled agent-based and flood modelling approach, Hydrol. Earth Syst. Sci., 24, 5329-5354, https://doi.org/10.5194/hess-24-5329-2020, 2020.

Aboelata, M. and Bowles, D.S.: LIFESim: A tool for estimating and reducing life-loss resulting from dam and levee failures, in: Proceedings of the Association of State Dam Safety Officials "Dam Safety 2008" Conference, Indian Wells, California, 7–11 September, 533-574, http://citeseerx.ist.psu.edu/viewdoc/summary?doi=10.1.1.155.2659, 2008.

Aerts, J.C., Botzen, W.J., Clarke, K.C., Cutter, S.L., Hall, J.W., Merz, B., Michel-Kerjan, E., Mysiak, J., Surminski, S. and Kunreuther, H.: Integrating human behaviour dynamics into flood disaster risk assessment, Nature Climate Change, 8, 193-199, https://doi.org/10.1038/s41558-018-0085-1, 2018.

Aerts, J.C.: Integrating agent-based approaches with flood risk models: a review and perspective, Water Security, 11, 1-9, https://doi.org/10.1016/j.wasec.2020.100076, 2020.

An, L., Grimm, V. and Turner II, B.L.: Meeting grand challenges in agent-based models, Journal of Artificial Societies and Social Simulation, 23, 13, https://doi.org/10.18564/jasss.4012, 2020.

802
803 Arrighi, C., Oumeraci, H. and Castelli, F.: Hydrodynamics of pedestrians' instability in floodwaters, Hydrol. Earth Syst. Sci.,
804 21, 515-531, https://doi.org/10.5194/hess-21-515-2017, 2017.
805
806 Becker, J.S., Taylor, H.L., Doody, B.J., Wright, K.C., Gruntfest, E. and Webber, D.: A review of people's behavior in and
807 around floodwater, Weather, Climate, and Society, 7, 321-332, https://doi.org/10.1175/WCAS-D-14-00030.1, 2015.
808
809 Bernardini, G. and Quagliarini, E.: How to account for the human motion to improve flood risk assessment in urban areas,
810 Water, 12, 1316, https://doi.org/10.3390/w12051316, 2020.
811
812 Bernardini, G., Postacchini, M., Quagliarini, E., Brocchini, M., Cianca, C. and D'Orazio, M.: A preliminary combined
813 simulation tool for the risk assessment of pedestrians' flood-induced evacuation, Environmental Modelling and Software, 96,
814 14-29, https://doi.org/10.1016/j.envsoft.2017.06.007, 2017.
815
816 Bernardini, G., Quagliarini, E., D'Orazio, M. and Brocchini, M.: Towards the simulation of flood evacuation in urban
817 scenarios: experiments to estimate human motion speed in floodwaters, Safety Science, 123, 104563,
818 https://doi.org/10.1016/j.ssci.2019.104563, 2020.
819
820 Bert, F.E., Rovere, S.L., Macal, C.M., North, M.J. and Podestá, G.P.: Lessons from a comprehensive validation of an agent
821 based-model: the experience of the pampas model of argentinean agricultural systems, Ecological Modelling, 273, 284-298,
822 https://doi.org/10.1016/j.ecolmodel.2013.11.024, 2014.
823
824 Bohannon, R.W. and Andrews, A.W.: Normal walking speed: a descriptive meta-analysis, Physiotherapy, 97, 182-189,
825 https://doi.org/10.1016/j.physio.2010.12.004, 2011.
826
827 Chanson, H., Brown, R. and McIntosh, D.: Human body stability in floodwaters: the 2011 flood in Brisbane CBD, in:
828 Proceedings of the 5th IAHR International Symposium on Hydraulic Structures, University of Queensland, Brisbane,
829 Australia, 25-27 June 2014, 1-9, https://doi.org/10.14264/uql.2014.48, 2014.
830
831 Costabile, P., Costanzo, C., De Lorenzo, G. and Macchione, F.: Is local flood hazard assessment in urban areas significantly
832 influenced by the physical complexity of the hydrodynamic inundation model?, Journal of Hydrology, 580, 124231,
833 https://doi.org/10.1016/j.jhydrol.2019.124231, 2020.
834

Dawson, R.J., Peppe, R. and Wang, M..: An agent-based model for risk-based flood incident management, Natural Hazards, 59, 167-189, https://doi.org/10.1007/s11069-011-9745-4, 2011.

Disabled World: Adult Body Mass Index (BMI) Calculator and Table, Disabled World, https://www.disabled-world.com/calculators-charts/bmi.php, 2017.

Dobbs, R.J., Charlett, A., Bowes, S.G., O'neill, C.J.A., Weller, C., Hughes, J. and Dobbs, S.M.: Is this walk normal?, Age and Ageing, 22, 27-30, https://doi.org/10.1093/ageing/22.1.27, 1993.

Engineering ToolBox: Room Area per Person, available at: https://www.engineeringtoolbox.com/number-persons-buildings-d_118.html (last access: 15 January 2021), 2003.

Environment Agency: Flood Risks to People Methodology, Phase 2, outputs of the Flood and Coastal Defence R&D Programme, available at http://sciencesearch.defra.gov.uk/Document.aspx?Document=FD2321_3436_TRP.pdf (last access: 15 December 2020), 2006.

Environment Agency: Review of 2007 summer floods, Environment Agency, Almondsbury, Bristol, United Kingdom, available at: https://assets.publishing.service.gov.uk/government/uploads/system/uploads/attachment_data/file/292924/geho1107bnmi-e-e.pdf (last access: 22 January 2021), 2007.

Flood and coastal erosion risk management policy statement, Department for Environment, Food and Rural Affairs, available at: https://www.gov.uk/government/publications/flood-and-coastal-erosion-risk-management-policy-statement (last access: 03 March 2021), 14 July 2020.

Football Webpages: Sheffield Wednesday, https://www.footballwebpages.co.uk/sheffield-wednesday, last access: 03 March 2021.

Hamilton, K., Demant, D., Peden, A.E. and Hagger, M.S.: A systematic review of human behaviour in and around floodwater, International Journal of Disaster Risk Reduction, 47, 101561, https://doi.org/10.1016/j.ijdrr.2020.101561, 2020.

Helbing, D. and Molnar, P.: Social force model for pedestrian dynamics, Phys. Rev. E, 51, 4282, https://doi.org/10.1103/PhysRevE.51.4282, 1995.

869 Ishigaki, T., Kawanaka, R., Onishi, Y., Shimada, H., Toda, K. and Baba, Y.: Assessment of safety on evacuating route during
870 underground flooding, in: Advances in Water Resources and Hydraulic Engineering: Proceedings of 16th IAHR-APD
871 Congress and 3rd Symposium of IAHR-ISHS, Springer, Berlin, Heidelberg, 141-146, https://doi.org/10.1007/978-3-540-
872 89465-0, 2009.
873
874 Jiang, Y., Chen, B., Li, X. and Ding, Z.: Dynamic navigation field in the social force model for pedestrian evacuation, Applied
875 Mathematical Modelling, 80, 815-826, https://doi.org/10.1016/j.apm.2019.10.016, 2020.
876
877 Karmakharm, T., Richmond, P. and Romano, D.M.: Agent-based large scale simulation of pedestrians with adaptive realistic
878 navigation vector fields, Theory and Practice of Computer Graphics, 10, 67-74,
879 http://dx.doi.org/10.2312/LocalChapterEvents/TPCG/TPCG10/067-074, 2010.
880
881 Kvočka, D., Falconer, R.A. and Bray, M.: Flood hazard assessment for extreme flood events, Natural Hazards, 84, 1569-1599,
882 https://doi.org/10.1007/s11069-016-2501-z, 2016.
883
884 Lange, D.: Share of people who have attended at least two live sports events in the last year in England from May 2018 to May
885 2020 by age, available at: https://www.statista.com/statistics/783771/live-sports-events-spectators-england-by-by-age/ (last
886 access 03 March 2021), 2020.
887
888 Lee, H.K., Hong, W.H. and Lee, Y.H.: Experimental study on the influence of water depth on the evacuation speed of elderly
889 people in flood conditions, International Journal of Disaster Risk Reduction, 39, 101198,
890 https://doi.org/10.1016/j.ijdrr.2019.101198, 2019.
891
892 Li, M., Wei, Y. and Xu, Y.: A route navigation algorithm for pedestrian simulation based on grid potential field, Advances in
893 Mechanical Engineering, 11, 1–13, https://doi.org/10.1177%2F1687814019897831, 2019.
894
895 Lin, J., Zhu, R., Li, N. and Becerik-Gerber, B.: Do people follow the crowd in building emergency evacuation? A cross-cultural
896 immersive virtual reality-based study, Advanced Engineering Informatics, 43, 101040,
897 https://doi.org/10.1016/j.aei.2020.101040, 2020.
898
899 Liu, X. and Lim, S.: Integration of spatial analysis and an agent-based model into evacuation management for shelter
900 assignment and routing, Journal of spatial science, 61, 283-298, https://doi.org/10.1080/14498596.2016.1147393, 2016.
901

902 Lumbroso, D. and Davison, M.: Use of an agent-based model and Monte Carlo analysis to estimate the effectiveness of
903 emergency management interventions to reduce loss of life during extreme floods, Journal of Flood Risk Management, 11,
904 S419-S433, https://doi.org/10.1111/jfr3.12230, 2018.
905
906 Lumbroso, D. and Di Mauro, M.: Recent developments in loss of life and evacuation modelling for flood event management
907 in the UK, WIT Transactions on Ecology and the Environment, 118, 263-272, https://doi.org/10.2495/FRIAR080251, 2008.
908
909 Lumbroso, D.M., Sakamoto, D., Johnstone, W.M., Tagg, A.F. and Lence, B.J.: Development of a life safety model to estimate
910 the risk posed to people by dam failures and floods, Dams and Reservoirs, 21, 31-43,
911 https://doi.org/10.1680/dare.2011.21.1.31, 2011.
912
913 Mas, E., Koshimura, S., Imamura, F., Suppasri, A., Muhari, A. and Adriano, B.: Recent advances in agent-based tsunami
914 evacuation simulations: case studies in Indonesia, Thailand, Japan and Peru, Pure and Applied Geophysics, 172, 3409-3424,
915 https://doi.org/10.1007/s00024-015-1105-y, 2015.
916
917 Matsuo, K., Natainia, L. and Yamada, F.: Flood and evacuation simulations for urban flooding, 5th International Conference
918 on Flood Management, Tokyo, Japan, 27-29 September 2011, 391-398, 2011.
919
920 McClymont, K., Morrison, D., Beevers, L. and Carmen, E.: Flood resilience: a systematic review, Journal of Environmental
921 Planning and Management, 63, 1151-1176, https://doi.org/10.1080/09640568.2019.1641474, 2020.
922
923 Milanesi, L., Pilotti, M. and Ranzi, R.: A conceptual model of people's vulnerability to floods, Water Resour. Res., 51, 182-
924 197, https://doi.org/10.1002/2014WR016172, 2015.
925
926 Minegishi, Y. and Takeichi, N.: Design guidelines for crowd evacuation in a stadium for controlling evacuee accumulation
927 and sequencing, Japan Architectural Review, 1, 471-485, https://doi.org/10.1002/2475-8876.12042, 2018.
928
929 Moftakhari, H.R., AghaKouchak, A., Sanders, B.F., Allaire, M. and Matthew, R.A.: What is nuisance flooding? Defining and
930 monitoring an emerging challenge, Water Resour. Res., 54, 4218-4227, https://doi.org/10.1029/2018WR022828, 2018.
931
932 Mohler, B.J., Thompson, W.B., Creem-Regehr, S.H., Pick, H.L. and Warren, W.H.: Visual flow influences gait transition
933 speed and preferred walking speed, Experimental Brain Research, 181, 221-228, https://doi.org/10.1007/s00221-007-0917-0,
934 2007.
935

936 Musolino, G., Ahmadian, R., Xia, J. and Falconer, R.A.: Mapping the danger to life in flash flood events adopting a mechanics
937 based methodology and planning evacuation routes, Journal of Flood Risk Management, 13, e12627,
938 https://doi.org/10.1111/jfr3.12627, 2020.
939
940 Netzel, L.M., Heldt, S., Engler, S. and Denecke, M.: The importance of public risk perception for the effective management
941 of pluvial floods in urban areas: a case study from Germany, Journal of Flood Risk Management [early view],
942 https://doi.org/10.1111/jfr3.12688, 2021.
943
944 Polhill, J.G., Sutherland, L.A. and Gotts, N.M.: Using qualitative evidence to enhance an agent-based modelling system for
945 studying land use change, Journal of Artificial Societies and Social Simulation, 13, 10, https://doi.org/10.18564/jasss.1563,
946 2010.
947
948 Prentice, A.M.: Body mass index standards for children: are useful for clinicians but not yet for epidemiologists, Br. Med. J.
949 (Clin. Res. Ed.), 317, 1401-1402, https://dx.doi.org/10.1136%2Fbmj.317.7170.1401, 1998.
950
951 Pugh, W.: Severe flooding near Hillsborough will not stop Sheffield Wednesday's game against Swansea being played
952 tomorrow despite homes nearby being evacuated, https://www.thesun.co.uk/sport/football/10303677 (last access: 03 March
953 2021), 2019.
954
955 Rufat, S., Fekete, A., Armaş, I., Hartmann, T., Kuhlicke, C., Prior, T., Thaler, T. and Wisner, B.: Swimming alone? Why
956 linking flood risk perception and behavior requires more than “it's the individual, stupid”, WIREs Water, 7, e1462,
957 https://doi.org/10.1002/wat2.1462, 2020.
958
959 Shirvani, M, Kesserwani, G, Richmond, P.: Agent-based simulator of dynamic flood-people interactions, Journal of Flood
960 Risk Management [early view], e12695, https://doi.org/10.1111/jfr3.12695, 2021.
961
962 Shirvani, M, Kesserwani, G.: Flood-pedestrian simulator, Zenodo [code], https://doi.org/10.5281/zenodo.4564288, 2021a.
963
964 Shirvani, M, Kesserwani, G.: Outputs of the flood-pedestrian simulator applied to the flooded shopping centre and
965 Hillsborough Stadium test cases, Zenodo [data set], https://doi.org/10.5281/zenodo.4576906, 2021b.
966
967 Shirvani, M., Kesserwani, G. and Richmond, P.: Agent-based modelling of pedestrian responses during flood emergency:
968 mobility behavioural rules and implications for flood risk analysis, Journal of Hydroinformatics, 22, 1078-1092,
969 https://doi.org/10.2166/hydro.2020.031, 2020.

970
971 Shirvani, M.: Flood-pedestrian simulator video demos, TIB AV-Portal [video], https://doi.org/10.5446/51547, 2021.
972
973 Statista Research Department: Europe: distribution of football fans in 2016, by country and gender, available at:
974 https://www.statista.com/statistics/658959/europe-football-fans-by-country-and-gender/ (last access 03 March 2021), 2016.
975
976 Still, G.K.: Crowd Safety and Crowd Risk Analysis, Crowd Risk Analysis Ltd, available at:
977 https://www.gkstill.com/Support/crowd-density/CrowdDensity-1.html (last access: 03 March 2021), 2019.
978
979 Teichtahl, A.J., Wluka, A.E., Strauss, B.J., Wang, Y., Berry, P., Davies-Tuck, M. and Cicuttini, F.M.: The associations between
980 body and knee height measurements and knee joint structure in an asymptomatic cohort, BMC Musculoskeletal Disorders, 13,
981 1-7, https://doi.org/10.1186/1471-2474-13-19, 2012.
982
983 Toor, A., Happer, A., Overgaard, R. and Johal, R.: Real world walking speeds of young pedestrians, SAE International, 110,
984 1106-1114, http://www.jstor.org/stable/44730963, 2001.
985
986 UK population by ethnicity, Office for National Statistics [data set], available at: https://www.ethnicity-facts-
987 figures.service.gov.uk/uk-population-by-ethnicity (last access: 03 March 2021), 2018.
988
989 Willis, T., Wright, N. and Sleigh, A.: Systematic analysis of uncertainty in 2D flood inundation models, Environmental
990 Modelling and Software, 122, 104520, https://doi.org/10.1016/j.envsoft.2019.104520, 2019.
991
992 Xia, J., Falconer, R.A., Wang, Y. and Xiao, X.: New criterion for the stability of a human body in floodwaters, Journal of
993 Hydraulic Research, 52, 93-104, https://doi.org/10.1080/00221686.2013.875073, 2014.
994
995 Zhu, X., Dai, Q., Han, D., Zhuo, L., Zhu, S., and Zhang, S.: Modelling the high-resolution dynamic exposure to flooding in a
996 city region, Hydrol. Earth Syst. Sci., 23, 3353–3372, https://doi.org/10.5194/hess-23-3353-2019, 2019.
997
998 Zhuo, L. and Han, D.: Agent-based modelling and flood risk management: a compendious literature review, Journal of
999 Hydrology, 591, 125600, https://doi.org/10.1016/j.jhydrol.2020.125600, 2020.
1000